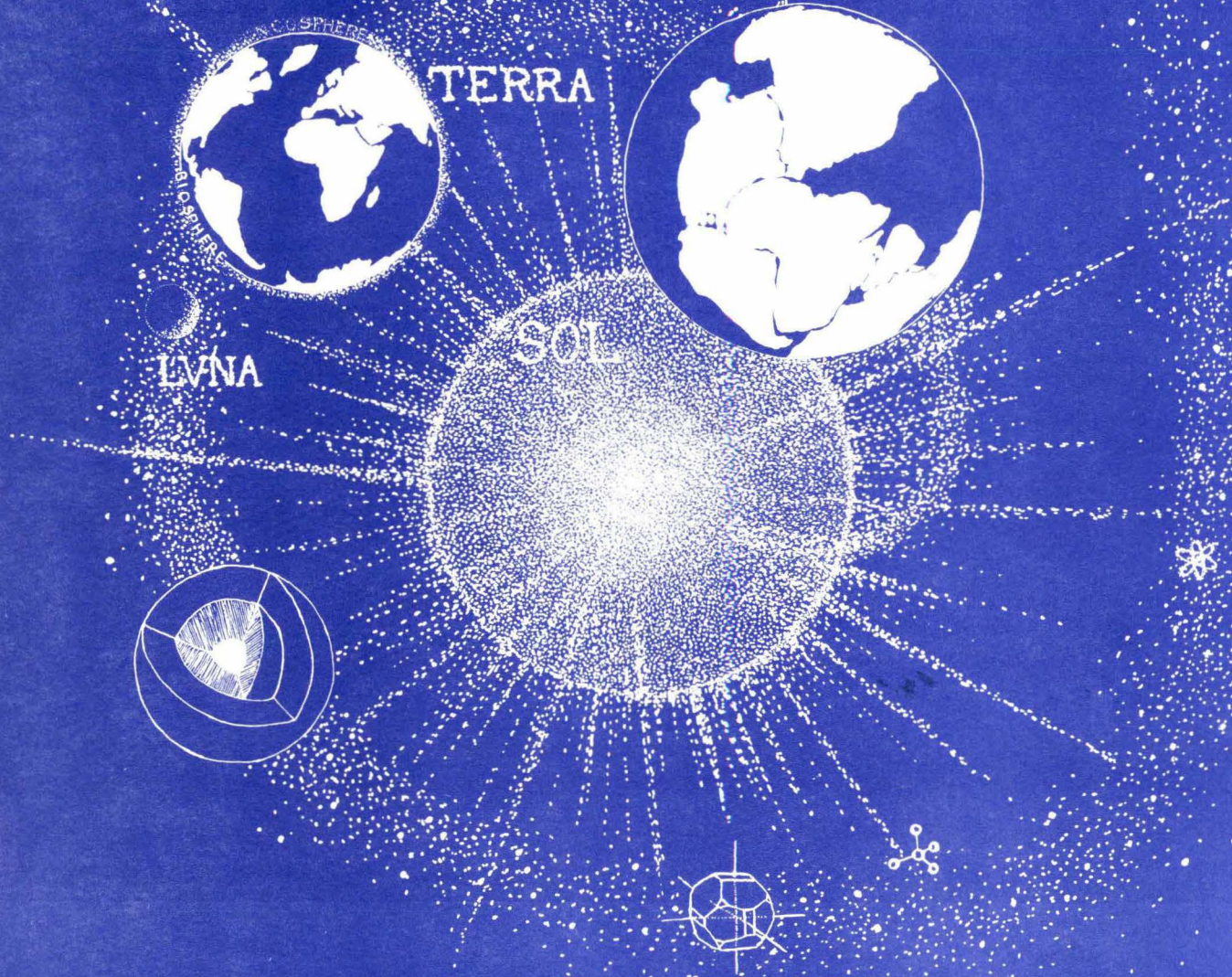


STONY BROOK



**The Apollo 17 Drill Core: Characterization of the
Mineral and Lithic Component (Sections 70007, 70008, 70009)**

by

**D. T. Vaniman and J. J. Papike
Department of Earth and Space Sciences
State University of New York
Stony Brook, New York 11794**

In press, Proceedings of the Eighth Lunar and Planetary Conference, Houston, Texas.

July, 1977
CORE CORPS

ABSTRACT

The > 0.02 mm lithic and mineral fragments in the upper three segments of the Apollo 17 drill core (70007, 70008, 70009) reflect a dominant subfloor mare basalt source. The mare source was most likely composed of a fractionated series ranging from quenched olivine porphyritic ilmenite basalt (OPIB) to plagioclase poikilitic ilmenite basalt (PPIB). The upper part of the drill core (70009) has been disturbed since emplacement, but the core still preserves a stratigraphy of pyroxene grains ranging from fractionated, Fe-rich PPIB pyroxene at the surface (70008, 70009) to quench-composition OPIB pyroxene at depth (70007). The coarse-grained soils of 70008 have been attributed to an overturned flap from Camelot Crater, and the basalt stratigraphy of the upper core may be an inverted flow sequence excavated from a subfloor basalt unit. Other high-Ti and very low-Ti (VLT) basalts are present, but rare, in the drill core. The highland lithic component consists of anorthositic gabbro and noritic rock types characteristic of North and South Massifs. The anorthositic component predominates over the noritic in the upper drill core (70009, 70008) but noritic compositions become more abundant lower in the drill core (70007), where the mare component decreases and the highlands component increases. Highland lithic fragments > 0.02 mm are a minor component (0-2.5%) throughout these three segments of the drill core. Increase of the highlands component in 70007 is principally seen as an increase in Mg-rich olivine grains ($> \text{Fo}_{80}$) at the bottom of 70007. Calcic feldspar does not increase significantly along with Mg-rich olivine, indicating that the highland mineral fragments in 70007 come from mafic rather than anorthositic sources.

INTRODUCTION

The Apollo 17 drill core is the deepest soil column (~ 295 cm) returned from the Moon. The core sample was taken within the dark mare soils of the Taurus-Littrow Valley, about one crater diameter (400 m) SE of Camelot/and NW of the "Central Cluster" craters which Arvidson et al. (1976) described as secondary craters from Tycho. Studies of neutron fluence suggest that the entire drill core was deposited less than 200 m.y. ago (Curtis and Wasserburg, 1975); the surrounding craters are as old or younger. Rocks sampled within the Central Cluster have consistent rare gas ages of about 100 m.y. (Arvidson et al., 1976), the apparent date of soil disturbance due to Central Cluster cratering (Wolfe et al., 1975). Camelot Crater may be the same age or slightly younger than the Central Cluster craters (Arvidson et al., 1975, and Taylor et al., 1977).

Taylor et al. (1977) used cratering models to attribute all of the soil in the upper drill core (70007, 70008, 70009) to Camelot and Central Cluster ejecta. The coarse-grained layer that comprises 70008 is believed to be an overturned flap of ejecta from Camelot Crater (LSPET, 1973; Duke and Nagle, 1975; Crozaz and Plachy, 1976). The underlying unit, 70007, could be part of the ~ 100 cm Camelot ejecta flap (Taylor et al., 1977), or the soil of 70007 may be attributed to one of the Central Cluster impacts (e.g., San Luis Rey; Taylor et al., 1977). The upper 19 cm of core material (70009) is made up of heavily irradiated surface soils which have filled a very young (~ 2 m.y.) shallow crater (Crozaz and Plachy, 1976, and Fruchter et al., 1976). The local impacts which have degraded and filled in this small crater may simply have reshuffled the original Camelot ejecta within 70009.

Duke and Nagle (1974) identified stratigraphic units within core segments 70007-70009 during the core dissection, and they developed an x-ray stratigraphy for the entire core. Both stratigraphies are shown in figure 1. A striking feature of the x-ray stratigraphy is a 60-cm thick coarse-grained unit that includes core segment 70008. In the simplified stratigraphies of later workers (Croaz and Plachy, 1976; Ali and Ehmann, 1977; Taylor et al., 1977; Papike et al., 1977) the coarse layer has been singled out as a distinctive immature unit of mare fragments capped by ~ 18-22 cm of mare-rich material which was reworked at ~ 2 m.y. The underlying soils (70007) are dominantly mare in composition, but grade downwards into an increasingly highlands-rich part of the drill core (Ali and Ehmann, 1977; Duke and Nagle, 1975).

Ali and Ehmann (1977) found that the increase in highlands material toward the base of 70007 was marked by decreasing Fe, Mg and increasing Al, Ca in the < 1 mm soil component. Taylor et al. (1977) and Papike et al. (1977) reported an increase in highland lithic fragments within 70007 relative to 70008 and 70009. Korotev (1976) analyzed size fractions of 70008 and developed chemical mixing models which show that mare components (basalt plus orange glass) account for ~ 90% of the 0.09-0.15 mm size fraction but only ~ 72% of the < 0.02 mm size fraction. The chemical models of Korotev also show that deficiency of mare material in the < 0.02 mm component of 70008 is made up by ~ 26% highlands material with the composition of anorthositic gabbro and noritic breccia in a 1:1 mix. The sparse highlands material (10%) in the 0.09-0.15 mm component is all anorthositic gabbro. In our companion paper (Vaniman and Papike, 1977c) we show that noritic lithic fragments as well as anorthositic gabbros are present in the 0.02-0.2 mm and > 0.2 mm size fractions of core segments 70007, 70008 and 70009.

Apparently both the anorthositic gabbro and noritic components are present in coarser and finer size fractions but the anorthositic gabbro is concentrated in the 0.09-0.15 mm fraction (Korotev, 1976). Clear glasses of the Apollo 17 core have the composition of anorthositic gabbro (Vaniman and Papike, 1977c) and are most abundant in the 0.09-0.15 mm size range. We suggest that these glasses account for the dominance of anorthositic gabbro in the highland component of Korotev's model soil for this size range.

LSPET (1973) originally characterized the important noritic breccia and anorthositic gabbro lithologies of the Apollo 17 highland massifs. Rhodes et al. (1974) have suggested that highland compositions in Apollo 17 valley floor soils are mixtures of these two lithologies. The subfloor mare basalt lithologies at the Apollo 17 site have been classified and discussed in a number of papers (LSPET, 1973; Papike et al., 1973, 1976; Rhodes et al., 1974; Longhi et al., 1974; Brown et al., 1975; Shih et al., 1975; Warner et al., 1975; Rhodes et al., 1976; Usselman et al., 1976; El Goresy and Ramdohr, 1977; Pratt et al., 1977). The Apollo 17 core and surface soils also contain small amounts of a very low Ti (VLT) mare basalt recently described by Vaniman and Papike (1977a) and Taylor et al. (1977). This paper discusses the relation of these rock types to the lithic and mineral fragments in the core thin sections.

ANALYTICAL METHODS

Modal Analyses

The modal data cited in this paper were obtained by characterization of 66,000 grid points on 35 polished thin sections. The methods of

modal analysis and detailed results are discussed in a companion paper by Vaniman and Papike (1977c).

Electron microprobe analysis of mineral and lithic fragments

All chemical analyses reported here were obtained on an ARL EMX-SM automated microprobe. Data were corrected by the procedures of Bence and Albee (1968) and Albee and Ray (1970). Apollo 17 orange glass beads in mount 74220,3a were used as an internal standard.

For the characterization of monomineralic fragments, four thin sections (70007,332; 70007,312; 70008,354 and 70009,288) were chosen at intervals of ~ 26 cm along the length of the drill core (Fig. 1). In order to obtain an unbiased sample of the major monomineralic components, analyses of pyroxene, olivine and feldspar were obtained in areas of $\sim 10 \text{ mm}^2$ in each of the four selected thin sections. All mineral fragments larger than $20 \mu\text{m}$ were analyzed in these representative areas. Multiple analyses were made of each pyroxene grain to account for chemical zoning.

Lithic fragments were analyzed in 18 thin sections. The total data base from microprobe analysis is 685 pyroxene analyses, 72 feldspar analyses, and 65 olivine analyses in monomineralic fragments plus 234 mineral analyses in 94 lithic fragments. Pyroxenes and olivines were analyzed for Si, Fe, Mg, Ca, Ti, Mn, Cr, Na and Al; feldspars were analyzed for Si, Fe, Mg, Ca, Na, K and Al; oxide minerals in lithic fragments were analyzed for Si, Fe, Mg, Ti, Mn, Cr and Al. All analyses are stored on magnetic tape in the lunar mineral data files at S.U.N.Y. Stony Brook. Representative mineral analyses are listed in Tables 2 to 8. Wherever possible, these analyses were selected to illustrate the limits of mineral composition within each lithic type. The full data set can be obtained from the authors.

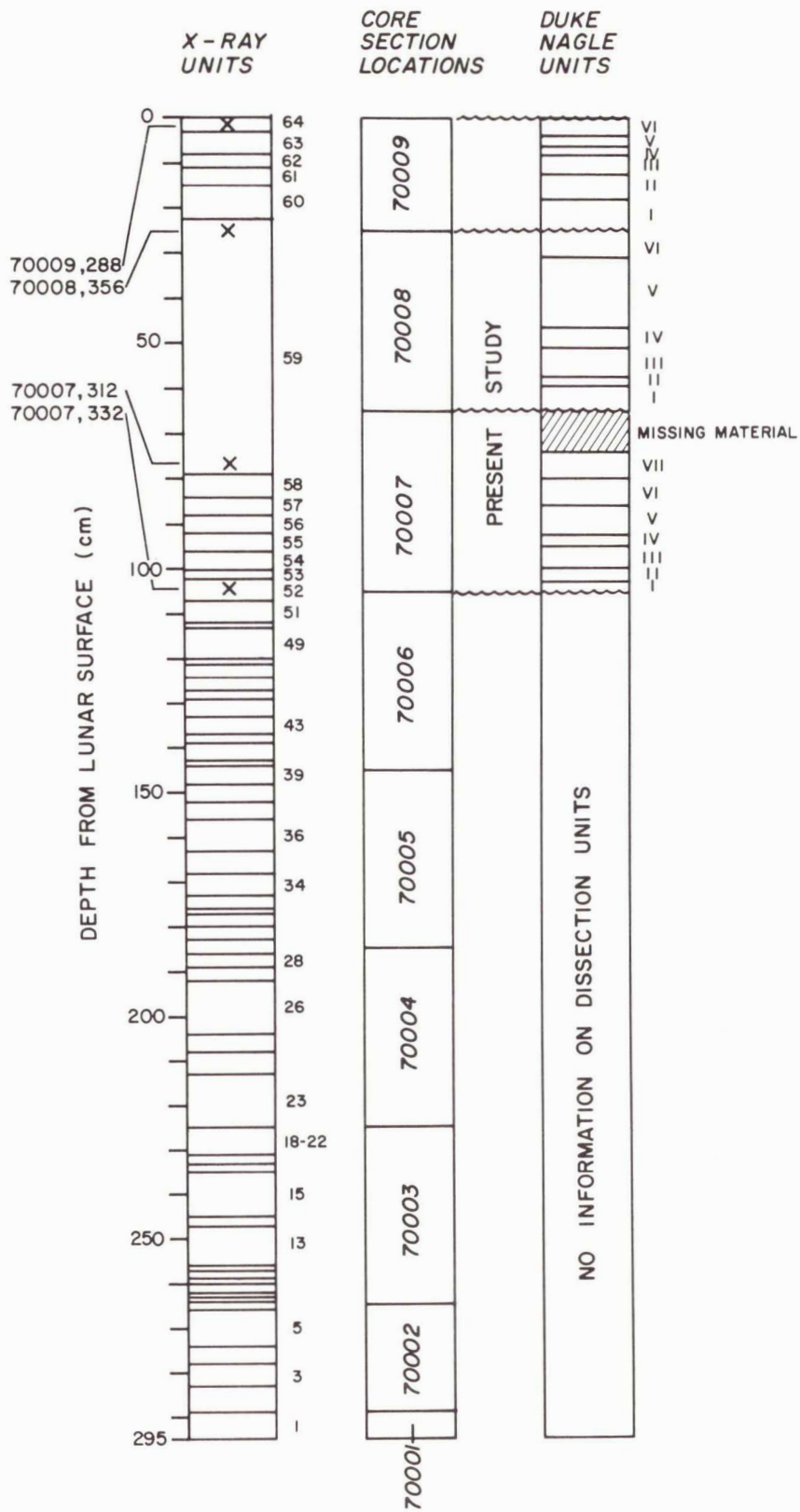


Fig. 1. X-ray stratigraphy, core segments and dissection stratigraphy of the Apollo 17 drill core (after Duke and Nagle, 1974). Locations are shown for the four polished thin sections (PTS) in which monomineralic fragments were analyzed.

THE LITHIC COMPONENTS

We have subdivided the drill core lithics into three major components: mare basalt, fused soil, and highland lithics. The fused soil component includes agglutinates and dark-matrix breccias. The major emphasis of this report concerns monomineralic fragments and mare and highland lithics; therefore, the fused soil component will not be dealt with in any detail.

In a companion paper (Vaniman and Papike, 1977c) we have distinguished three layers in the upper drill core. These three layers can be correlated with the x-ray units of Duke and Nagle (1974): the lower layer coincides with x-ray units 52-58, the central layer coincides with x-ray unit 59, and the top layer coincides with x-ray units 60-64 (ref. Fig. 1). Table 1a shows the percentage of 0.02-2.0 mm lithic fragments in the soils of these three layers. The complete data are discussed in the companion paper, but pertinent to this paper is the great abundance of plagioclase poikilitic basalt in the central layer, and the increase of noritic POIK+RNB lithics in the bottom layer.

The middle layer is distinguished by an abundance of coarse clasts (LSPET, 1973; Duke and Nagle, 1975; Crozaz and Plachy, 1976). Very coarse fragments > 2.0 mm were not point counted in our modal analysis, but each one of these fragments was individually characterized (Vaniman and Papike, 1977c). Table 1b shows that plagioclase poikilitic ilmenite basalts account for the increased abundance of these > 2.0 mm clasts in the central unit.

MARE LITHIC COMPONENT

Mare lithics of the three upper core sections are comprised of the common Apollo 17 very high-Ti (VHT) basalts (LSPET, 1973; Rhodes et al.,

Table 1a: Modal percentages of 0.02-2.0 mm lithic fragments in total soil.

	<i>Bottom:</i> <i>X-ray units 52-58</i>	<i>Center:</i> <i>X-ray unit 59</i>	<i>Top:</i> <i>X-ray units 60-64</i>
Intermediate and Olivine Porphyritic Ilmenite Basalt	2.0	1.4	1.1
Plagioclase Poikilitic Ilmenite Basalt	3.1	10.6	6.9
Other Mare Basalts	< 0.1	< 0.1	< 0.1
Feldspathic Basalt	<< 0.1	<< 0.1	<< 0.1
POIK/RNB	0.8	0.5	0.5
Anorthositic Gabbro	0.3	0.4	0.3
Light Matrix Breccia	0.1	0.6	0.2

Table 1b: Number of mare lithic fragments > 2.0 mm.

	<i>Bottom:</i> <i>X-ray units 52-58</i>	<i>Center:</i> <i>X-ray unit 59</i>	<i>Top:</i> <i>X-ray units 60-64</i>
Olivine Porphyritic Ilmenite Basalt	2	3	---
Intermediate Ilmenite Basalt	3	4	1
Plagioclase Poikilitic Ilmenite Basalt	4	15	4

1974), with minor amounts of another diabasic/ophitic high-Ti basalt and a very low-Ti (VLT) basalt type (Vaniman and Papike, 1977a,b and Taylor et al., 1977).

Longhi et al. (1974) suggested a near-surface fractionation relationship between the common VHT basalts and the "Apollo 11 type" high-Ti basalt at the Apollo 17 site. Several authors (Shih et al., 1975; Warner et al., 1975; Rhodes et al., 1976) have pointed out that trace-element contents complicate this scenario, requiring at least two or as many as five magma types. However, the presence of multiple magma types does not invalidate the fractionation scheme developed by Longhi et al. (1974).

The more abundant VHT basalts are commonly subdivided into two groups on the basis of texture (Papike et al., 1973; Brown et al., 1974): the vitrophyric to variolitic olivine porphyritic ilmenite basalts (OPIB) and the coarse-grained, plagioclase poikilitic ilmenite basalts (PPIB). Longhi et al. (1974) related the OPIB and PPIB basalts to the "Apollo 11 type" by the fractionation sequence:

Olivine porphyritic ilmenite basalt → plagioclase
poikilitic ilmenite basalt → Apollo 11 type low K
basalt.

This sequence satisfies major-element variation trends, but conflicts with trace-element data (Shih et al., 1975).

The trace-element evidence for several Apollo 17 magma types is tentatively supported by $^{40}\text{Ar}/^{39}\text{Ar}$ data. Olivine porphyritic ilmenite basalt may be ~ 80 m.y. older than plagioclase poikilitic ilmenite basalt (Schaeffer et al., 1976). However, this age difference is not necessarily correlated to basalt texture in any simple way throughout the Apollo 17 site. Usselman et al. (1976) and El Goresy and Ramdohr (1977) showed from paragenetic sequence and spinel compositions that OPIB crystallized at higher

f_{O_2} than the PPIB. The f_{O_2} variations may be further evidence of multiple magmas, or they may instead reflect separate cooling histories or a decrease in f_{O_2} with progressive crystallization within a single cooling unit.

The varied arguments for multiple high-Ti magmas at Taurus-Littrow have not been integrated. Evidence from $^{40}\text{Ar}/^{39}\text{Ar}$ dating by Schaeffer et al. (1976) suggests an age difference between OPIB and PPIB, but the minor element data of Rhodes et al. (1976) and Pratt et al. (1977) combine both textures within each of three magma types. Certainly the fractionation models of Papike et al. (1974) and Longhi et al. (1974) might operate on one or more of these magma types, and the genetic sequence(s)

OPIB → PPIB

or OPIB → PPIB → "Apollo 11 type"

may have been repeated in several flows of different ages.

The data presented in this paper are based on major-element microprobe analysis of mineral grains and minerals within lithic fragments. Problems of age and multiple magma types are, therefore, not considered. We believe that the petrography and composition of VHT basalts at Taurus-Littrow indicate that some of these basalts may be related by a fractionation sequence within at least one of the subfloor basalt flows.

Papike et al. (1974) studied the 2-4 mm basalt fragments in Apollo 17 surface soils and distinguished "Apollo 11 low K type" basalt on the basis of a diabasic/ophitic texture and pronounced Fe-enrichment of pyroxene. This Fe-enrichment of "Apollo 11 type" basalt has also been observed by Brown et al. (1975). However, within the drill core we find

that some basalt fragments with "Apollo 11 type texture" lack Fe-rich pyroxene, whereas the plagioclase poikilitic basalt fragments contain such Fe-rich pyroxene. The fragments with Apollo 11 type texture are rarest of all basalt types in the drill core. In this paper the term "diabasic/ophitic ilmenite basalt" is used for these rare fragments with Apollo 11 type texture but without the mineral composition of Apollo 11 low K basalt.

We use four categories to classify the high-Ti basalts. These categories are based on textural distinctions and mineral compositions. Three of these categories are used for the abundant olivine-normative VHT basalts (OPIB, intermediate, and PPIB); the fourth category is for the rare diabasic/ophitic ilmenite basalt. A fifth category is used for the new very low-Ti (VLT) basalt. These five rock types are described below:

(1) Olivine Porphyritic Ilmenite Basalt

OPIB occurs in a variety of fine-grained textures ranging from vitrophyric to intersertal (Fig. 2a). The presence of quenched glass is characteristic. Olivine + CrAl spinel + armalcolite are the common near-liquidus phases; the subsequent crystallization sequence is affected by f_{O_2} (Usselman *et al.*, 1976). Armalcolite, common in glassy OPIB, is lost by reaction with FeO from the melt to form ilmenite in the more equilibrated (i.e., more crystalline) OPIB fragments (Papike *et al.*, 1974). The olivine phenocrysts are skeletal or euhedral, slightly zoned (Fo_{65-77}) and occasionally rimmed by pyroxene. The characteristic pyroxene is skeletal or variolitic, high in CaO (Wo_{42-50}), Al_2O_3 (~ 9 wt.%) and TiO_2 (~ 6 wt.%). The high TiO_2

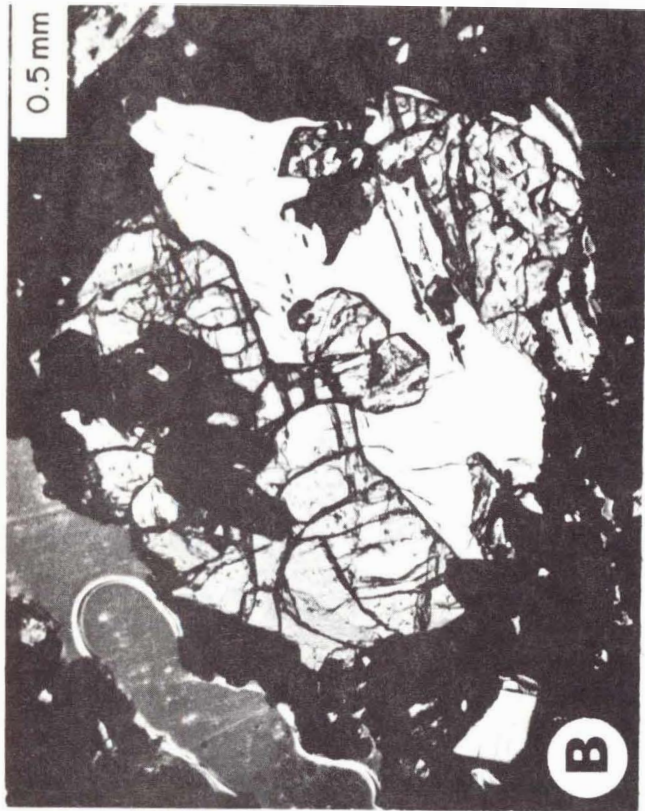


Fig. 2. Mare lithic fragments: (A) skeletal needles of armalcolite rimmed by ilmenite in OPIB. (B) ilmenite-pyroxene-feldspar of PPIB. (C) pyroxene-feldspar-cristobalite (c) of PPIB. (D) holocrystalline intermediate ilmenite basalt.

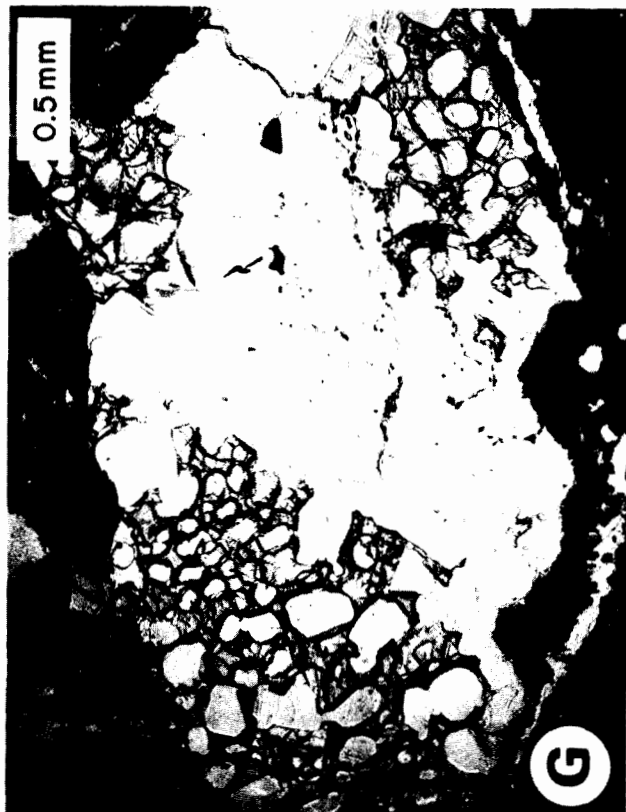
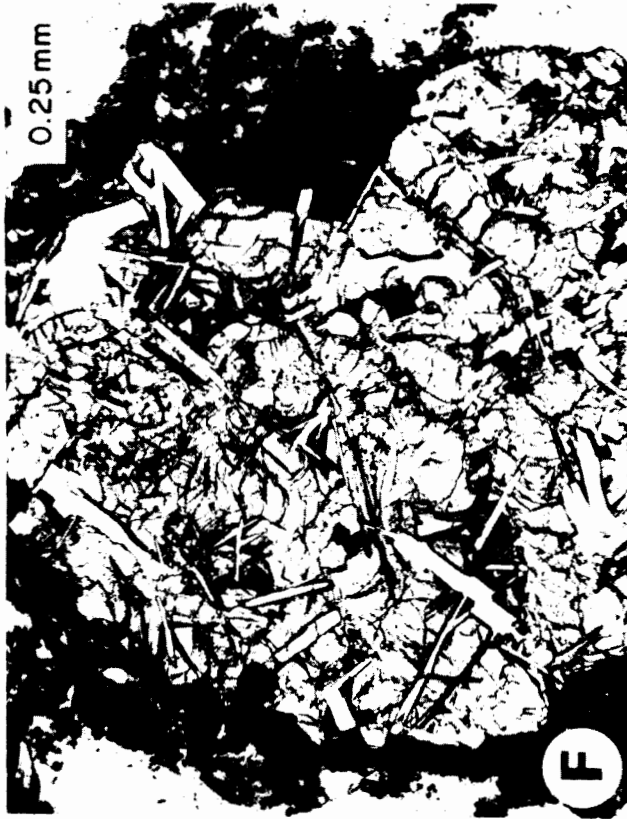


Fig. 2 (Cont.) Mare and highland lithic fragments: (E) diabasic/ophitic ilmenite basalt. (F) very low-Ti (VLT) basalt. (G) noritic POIK. (H) interstitial feldspathic basalt.

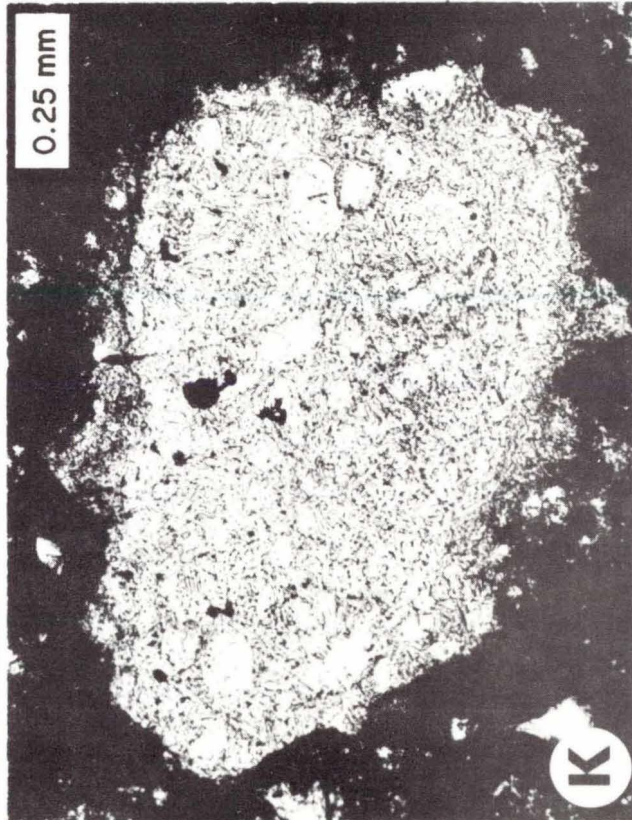
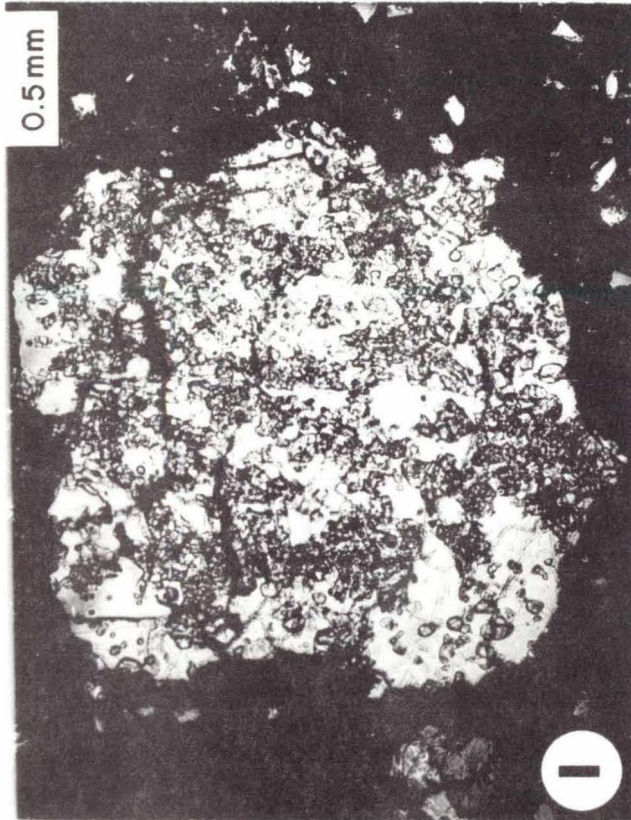
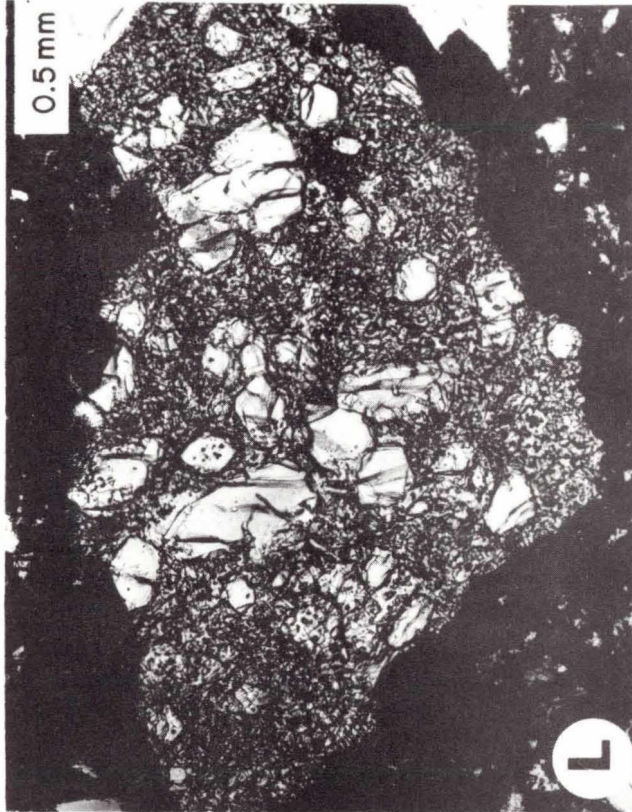
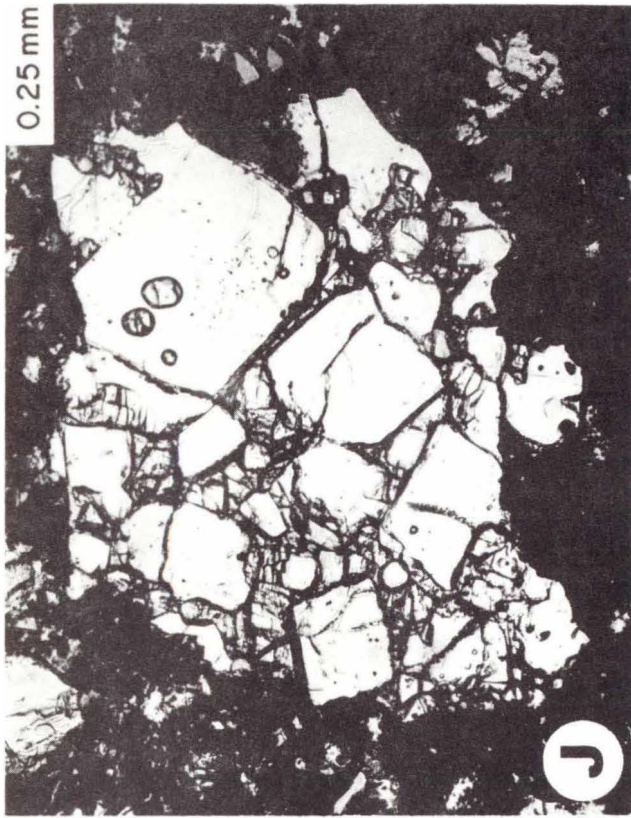


Fig. 2 (Cont.) Highland Lithic Fragments: (I) recrystallized noritic breccia. (J) anorthositic gabbro with inter-grain pyroxenes and rounded inclusions of olivine within feldspar. (K) anorthositic light matrix breccia. (L) Mg-rich recrystallized peridotite.

content gives OPIB pyroxenes a deep red, poorly pleochroic coloration. The Ti/Al ratio may be less than 1/2 (Fig. 5), and Al/Si ratios of ~ 0.25 at $\text{Fe}/(\text{Fe} + \text{Mg}) \sim 0.4$ (Fig. 7) are common in OPIB pyroxenes. All of these observations are consistent with those of Papike *et al.* (1974).

(2) *Intermediate Ilmenite Basalt*

The intermediate ilmenite basalts have a grain size (~ 0.2 mm) intermediate between OPIB and PPIB. The "intermediate" texture is holocrystalline equigranular, with elongate or skeletal ilmenite between subhedral pyroxene and anhedral plagioclase (Fig. 2d). Anhedral olivine ($\sim 1-4$ modal %; Fo_{65-75}) occurs as small rounded grains < 0.1 mm. Pyroxenes are zoned from the high Ca, Al, Ti compositions of OPIB pyroxenes toward the Ca-free pyroxene join. Characteristic features of the intermediate ilmenite basalts are: equigranular texture with bladed euhedral ilmenite; pyroxenes tinted red by high Ti content; high initial Ti + Al contents in pyroxene zoned to lower Ti + Al contents along the fixed ratio 1:2 (Fig. 5); and the absence of quench glass. Al/Si ratios > 0.15 in pyroxene are restricted to Mg-rich crystals with $\text{Fe}/(\text{Fe} + \text{Mg}) < 0.35$ (Fig. 7).

(3) *Plagioclase Poikilitic Ilmenite Basalt*

PPIB is characterized by large (~ 0.5 mm) poikilitic plagioclase grains enclosing rounded pyroxenes and ilmenite (Fig. 2b). Olivine is minor ($\sim 1\%$ modal or less), and cristobalite is a common minor phase (Fig. 2c). Metallic Fe and Fe sulfide in residual intergrain glasses indicate reducing conditions in the late-stage melt. Pyroxenes are pale or colorless, having lost most Ti to oxide phases. In PPIB, the Ca, Ti, Al depletion trend of intermediate ilmenite basalts is continued toward $\text{Wo}_{10}\text{En}_{60}\text{Fs}_{30}$; this is

the same PPIB pyroxene trend which was found by Papike et al. (1974) in the 2-4 mm surface component from the Apollo 17 site. However, the pyroxenes of PPIB in the drill core differ in having a prominent Fe-enrichment trend following Ca-depletion (Fig. 3). The difference between PPIB at the surface and in the drill core may be due to:

(a) A higher Fe:Ti ratio in PPIB of the drill core than in PPIB of the 2-4 mm surface component. This would permit greater Fe enrichment in pyroxene formed after ilmenite crystallization.

(b) More thorough fractionation in PPIB samples from the drill core, possibly including crystal settling of ilmenite. Removal of ilmenite would increase the Fe:Ti ratio of remaining liquid.

Ti and Al contents of PPIB pyroxenes are low, and are fixed by the ratio 1:2 (Fig. 5). The pyroxene Al/Si ratios are < 0.15 (Fig. 7).

(4) Diabasic/Ophitic Ilmenite Basalt

The diabasic/ophitic ilmenite basalts (Fig. 2e) have pyroxene compositions similar to intermediate ilmenite basalts of the core, but have more iron-rich olivines (Fo_{53-63} ; Fig. 3) and more calcic plagioclase (An_{90-95} ; Fig. 9). The high Fe content of olivine and the very calcic plagioclase fall outside the range of mineral compositions in the OPIB-PPIB series. The more abundant very high Ti basalts in the core may form a consistent OPIB--intermediate--PPIB fractionation series but the diabasic/ophitic high Ti basalts cannot fit into this trend.

PYROXENES MARE LITHIC COMPONENT

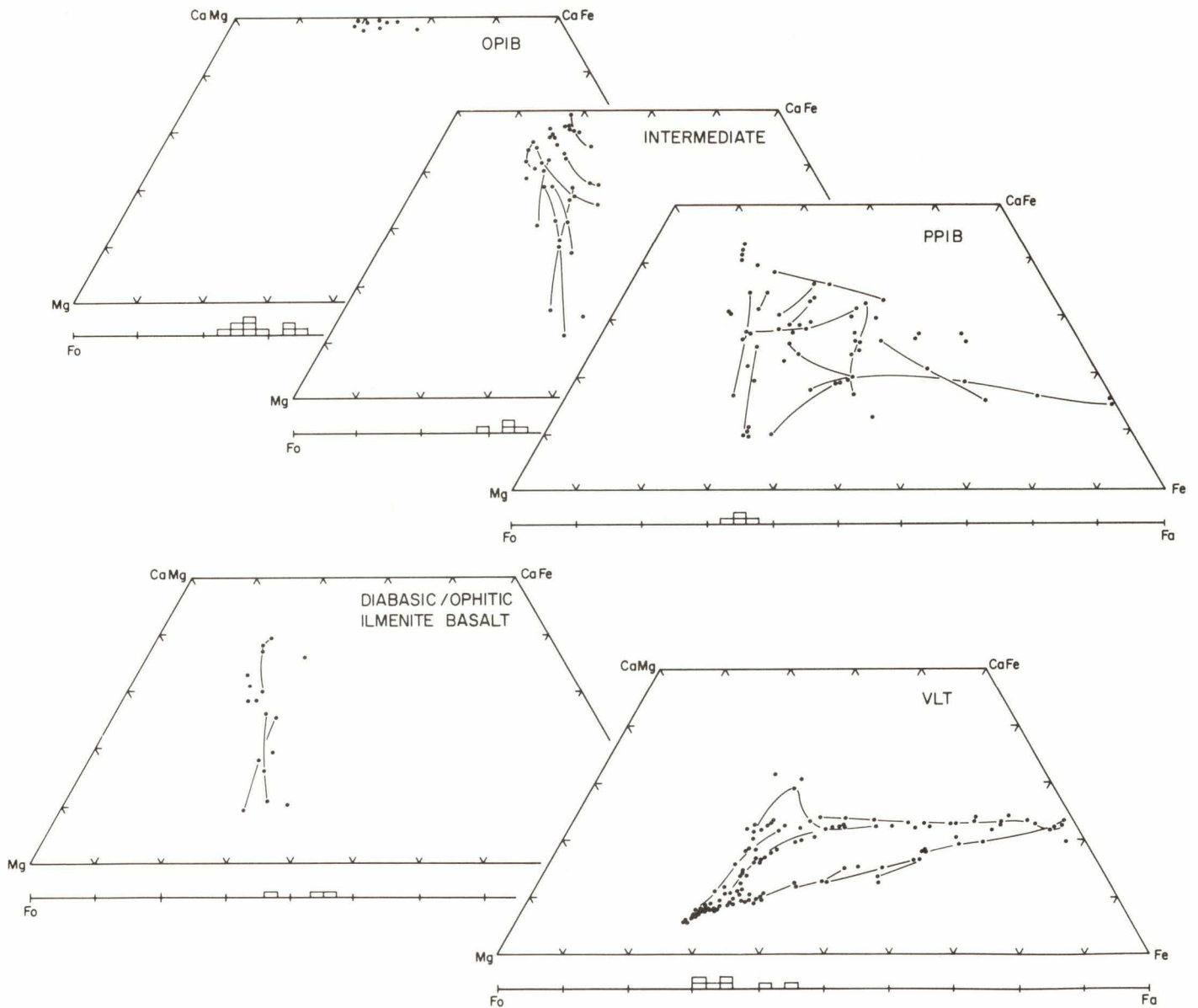


Fig. 3. Ca-Fe-Mg composition of pyroxene and Fe-Mg composition of olivine in mare lithic types.

PYROXENES HIGHLAND LITHIC COMPONENT

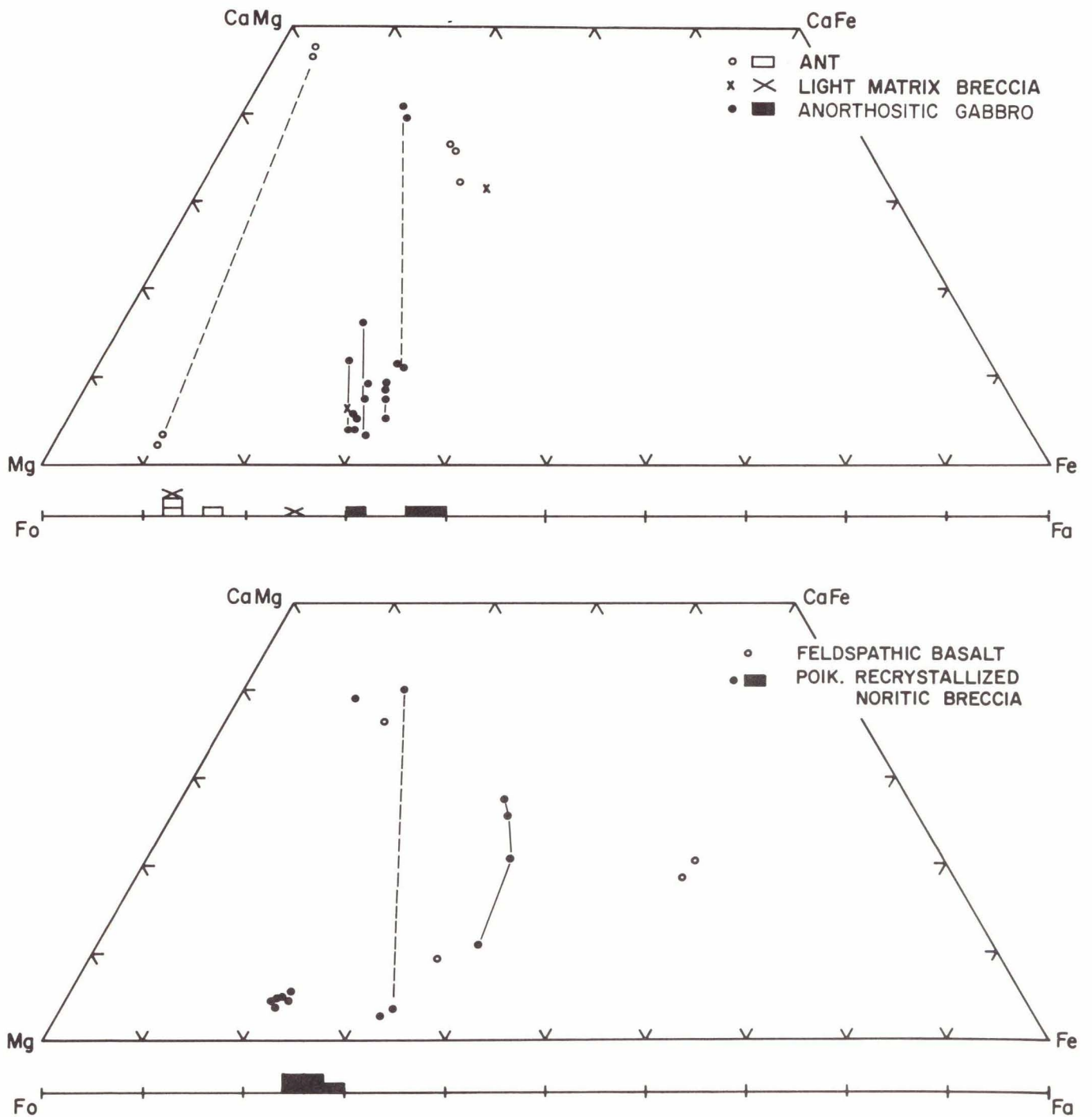


Fig. 4. Ca-Fe-Mg composition of pyroxene and Fe-Mg-composition of olivine in highland lithic types.

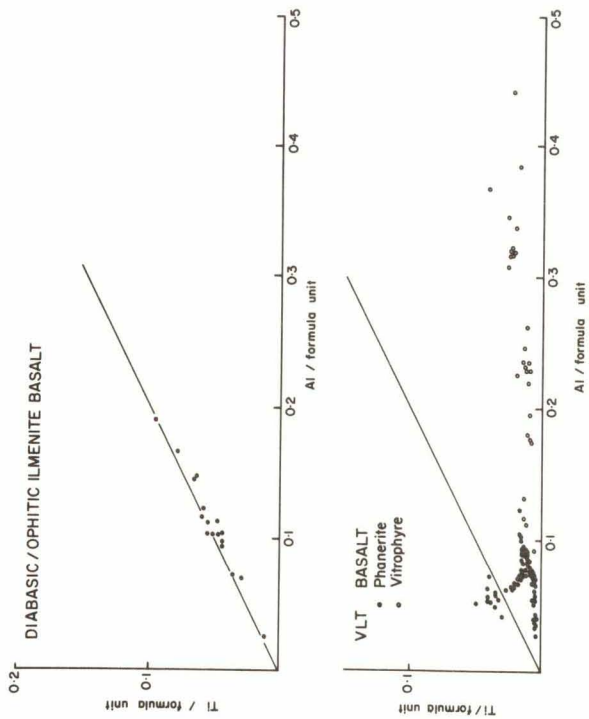
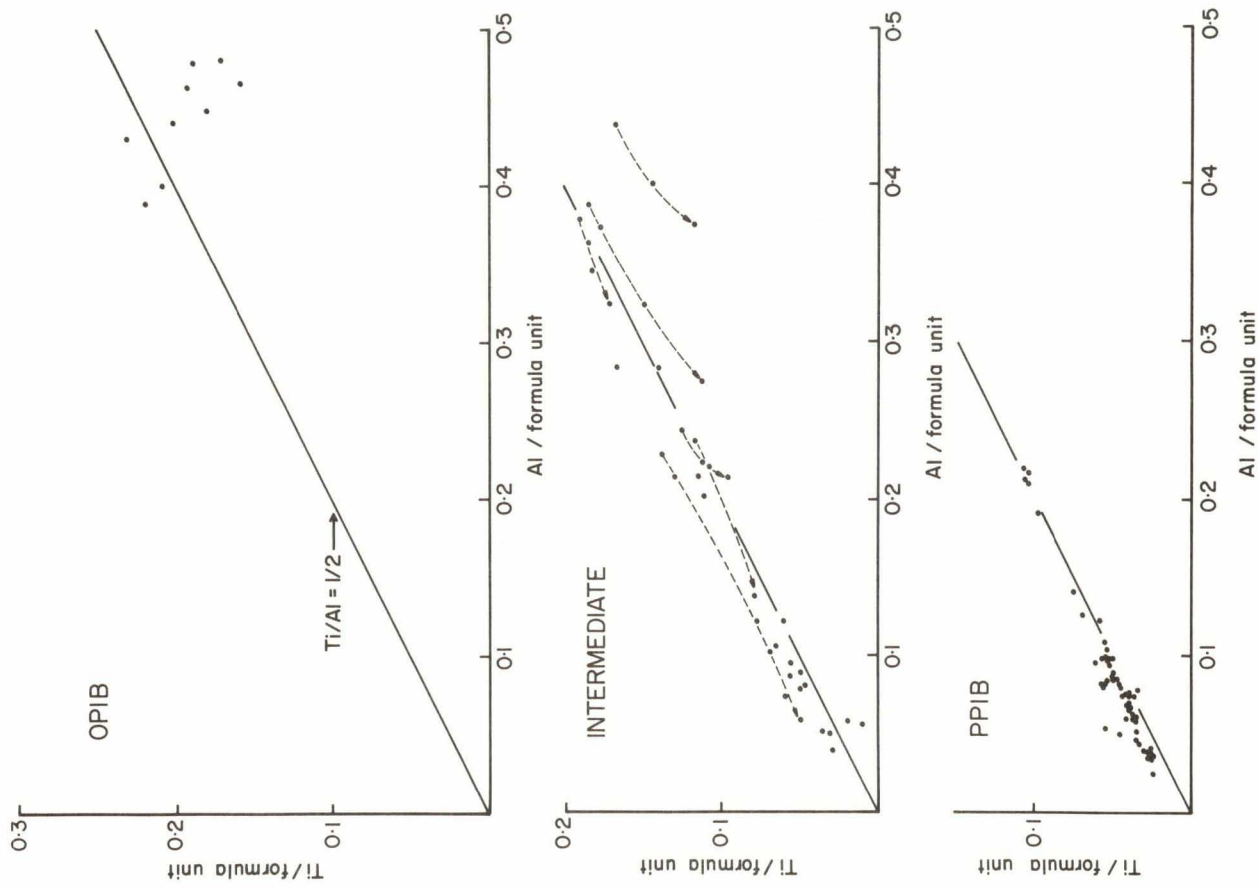


Fig. 5. Pyroxene Ti vs Al content, atoms per 6-oxygen formula unit: mare lithic types.

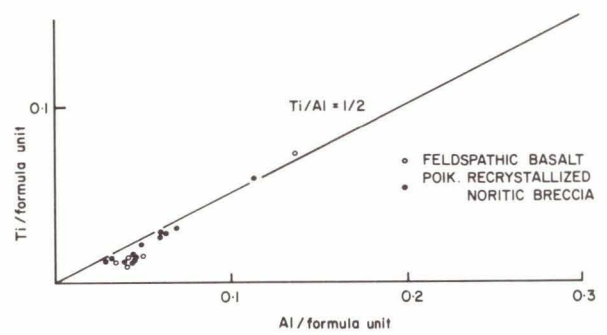
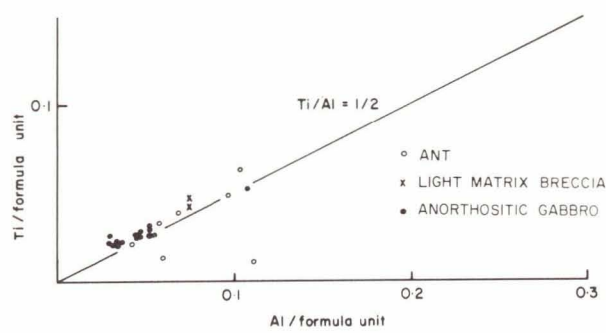


Fig. 6. Pyroxene Ti vs Al content, atoms per formula unit: Highland lithic types.

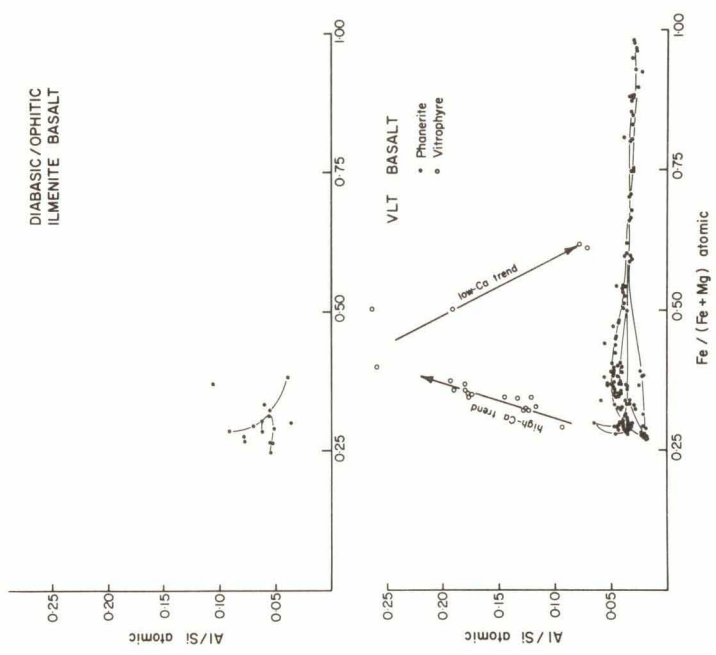
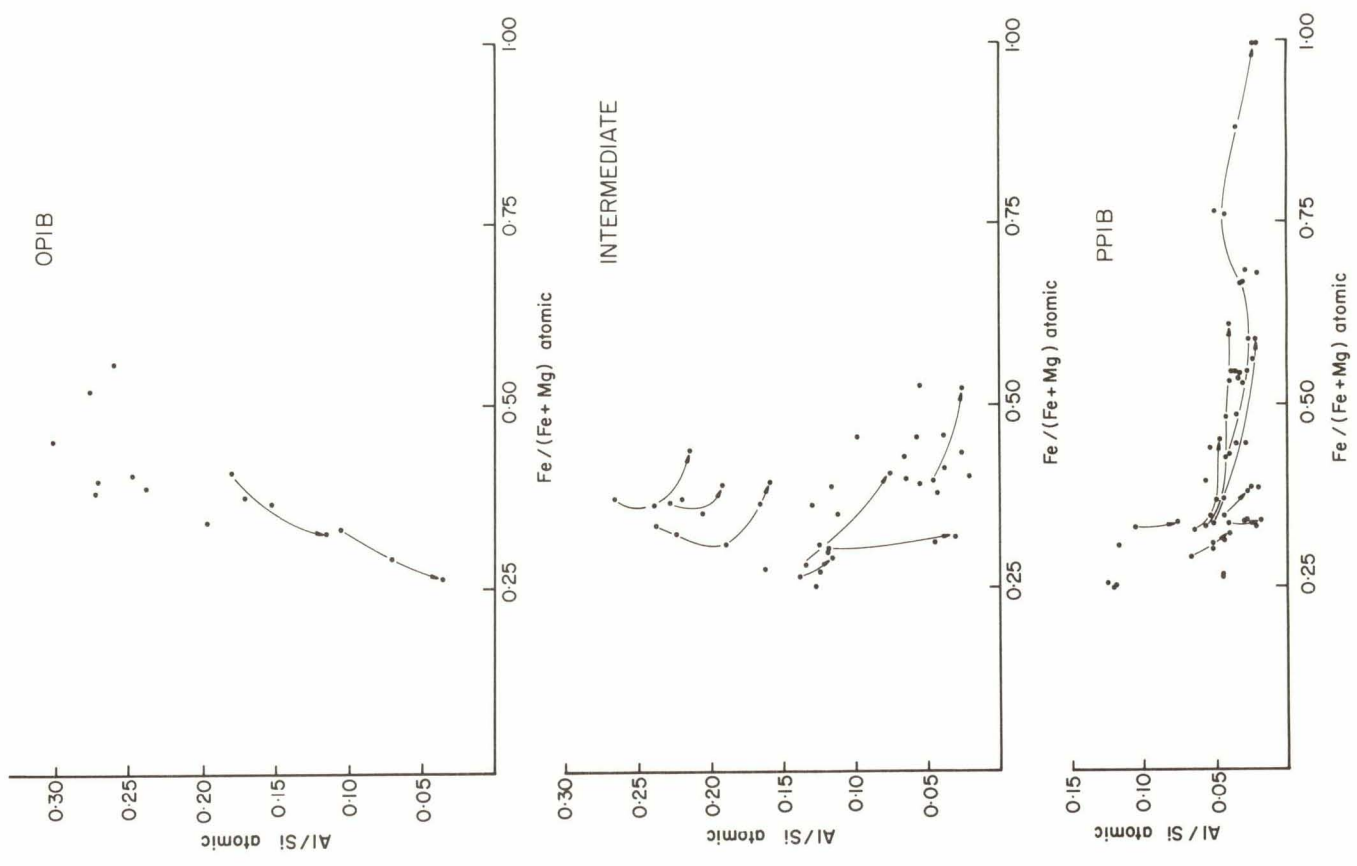


Fig. 7.
Atomic Al/Si vs atomic Fe/(Fe + Mg) in pyroxenes of mare lithic types.

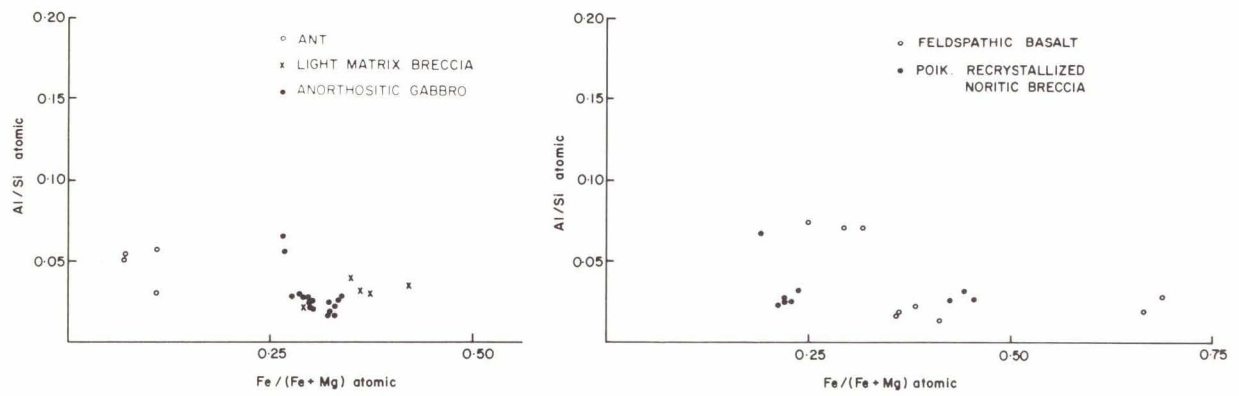


Fig. 8. Atomic Al/Si vs atomic Fe/(Fe + Mg) in pyroxenes of highland lithic types.

Pyroxene Compositions*, Mare Basalt Component

	1	2	3	4	5	6	7	8	9	10	11	12	13
SiO ₂	45.31	47.82	50.61	51.16	51.84	52.81	49.96	46.15	47.38	51.42	53.49	45.47	48.00
Al ₂ O ₃	7.33	4.93	1.96	0.91	1.34	0.97	1.37	0.77	4.26	1.66	1.04	1.55	7.32
TiO ₂	5.27	3.67	1.78	0.99	1.30	0.90	1.16	0.91	3.35	1.28	0.12	1.13	0.85
FeO	9.26	8.31	15.88	22.54	15.84	19.30	24.04	45.43	13.89	21.43	17.81	43.43	13.08
MnO	0.18	0.19	0.27	0.38	0.35	0.37	0.50	0.47	0.30	0.35	0.32	0.58	0.31
MgO	11.52	13.94	15.15	18.54	17.30	21.82	11.33	0.07	13.27	19.47	22.67	0.00	13.16
CaO	20.67	19.47	14.83	5.00	12.30	4.24	12.19	6.48	16.86	4.93	4.09	8.52	15.92
Na ₂ O	0.07	0.48	0.02	0.05	0.00	0.00	0.00	0.00	0.02	0.00	0.00	0.00	0.00
Cr ₂ O ₃	0.70	0.84	0.38	0.36	0.30	0.30	0.32	0.03	1.12	0.46	0.61	0.03	1.92
Total	100.31	99.65	100.88	99.93	100.57	100.71	100.87	100.31	100.45	101.00	100.15	100.71	100.56
Si	1.703	1.792	1.900	1.942	1.934	1.949	1.935	1.971	1.795	1.919	1.969	1.930	1.796
Al IV	0.325	0.218	0.087	0.040	0.059	0.042	0.063	0.039	0.190	0.073	0.031	0.070	0.204
Σ _{tet.} AlVI	2.000	2.000	1.987	1.982	1.993	1.991	1.998	2.000	1.985	1.992	2.000	2.000	2.000
AlVI	0.028	0.010	0.000	0.000	0.000	0.000	0.000	0.010	0.000	0.000	0.014	0.008	0.119
Ti	0.149	0.104	0.050	0.028	0.036	0.025	0.034	0.029	0.095	0.036	0.003	0.036	0.024
Fe	0.292	0.260	0.499	0.715	0.494	0.596	0.779	1.623	0.440	0.669	0.548	1.542	0.409
Mn	0.006	0.006	0.009	0.012	0.011	0.012	0.016	0.017	0.010	0.011	0.010	0.021	0.010
Mg	0.646	0.779	0.848	1.049	0.962	1.200	0.654	0.004	0.749	1.083	1.243	0.000	0.734
Ca	0.833	0.782	0.597	0.203	0.492	0.168	0.506	0.297	0.684	0.197	0.161	0.388	0.638
Na	0.005	0.035	0.002	0.004	0.000	0.000	0.000	0.000	0.001	0.000	0.000	0.000	0.000
Cr	0.021	0.025	0.011	0.011	0.009	0.009	0.010	0.001	0.034	0.013	0.018	0.001	0.057
Σ _{oct. and VIII} Cations	1.980	2.001	2.016	2.022	2.004	2.010	1.999	1.981	2.013	2.009	1.997	1.996	1.991
Σ _{Cations}	3.980	4.001	4.003	4.004	3.997	4.001	3.997	3.981	3.998	4.001	3.997	3.996	3.991
Wb	46.9	42.8	30.6	10.3	25.1	8.5	25.9	15.3	36.3	10.1	8.2	19.9	35.6
En	36.4	42.6	43.4	53.0	49.1	60.8	33.4	0.2	39.8	55.2	63.4	0.0	41.0
Fs	16.7	14.6	26.0	36.7	25.8	30.7	40.7	84.5	23.9	34.7	28.4	80.1	23.4

* All analyses normalized to six oxygens; Column (1): Olivine porphyritic ilmenite basalt; Columns (2-4): Intermediate texture ilmenite basalt; Columns (5-8): Plagioclase poikilitic ilmenite basalt; Columns (9-10): Diabasic/ophitic ilmenite basalt; Columns (11-12): Very low-Ti (VLT) basalt; Column (13): Very low-Ti (VLT) vitrophyre.

Table 3

Pyroxene Compositions*: Highland Component

	1	2	3	4	5	6	7	8	9
SiO ₂	50.76	53.30	51.10	52.81	51.06	54.30	51.24	51.96	49.74
Al ₂ O ₃	3.10	1.21	1.71	0.83	1.66	0.97	1.37	1.44	0.76
TiO ₂	1.85	0.86	1.70	0.98	1.68	0.83	1.00	1.51	0.40
FeO	10.03	18.53	13.54	17.44	13.81	13.43	20.12	20.27	31.80
MnO	0.19	0.31	0.21	0.37	0.19	0.20	0.35	0.36	0.47
MgO	15.44	21.82	14.06	22.24	13.91	27.58	14.08	20.10	8.89
CaO	18.32	3.57	17.42	5.55	17.25	2.23	12.07	5.53	8.59
Na ₂ O	0.05	0.00	0.03	0.00	0.06	0.00	0.00	0.00	0.00
Cr ₂ O ₃	0.66	0.40	0.73	0.38	0.64	0.51	0.62	0.34	0.46
Total	100.40	100.00	100.50	100.60	100.26	100.05	100.85	101.51	101.11
Si	1.882	1.967	1.919	1.944	1.923	1.950	1.943	1.921	1.971
Al ^{IV}	0.118	0.033	0.076	0.036	0.074	0.041	0.061	0.063	0.036
Σ _{tet.}	2.000	2.000	1.995	1.980	1.997	1.991	2.000	1.984	2.000
Al ^{VI}	0.018	0.021	0.000	0.000	0.000	0.000	0.004	0.000	0.007
Ti	0.052	0.024	0.048	0.027	0.048	0.022	0.029	0.042	0.012
Fe	0.311	0.572	0.425	0.537	0.435	0.404	0.639	0.627	1.054
Mn	0.006	0.010	0.007	0.011	0.006	0.006	0.011	0.011	0.016
Mg	0.853	1.200	0.787	1.220	0.781	1.476	0.796	1.108	0.525
Ca	0.728	0.141	0.701	0.219	0.696	0.086	0.491	0.219	0.365
Na	0.003	0.000	0.002	0.000	0.005	0.000	0.000	0.000	0.000
Cr	0.020	0.012	0.022	0.011	0.019	0.014	0.019	0.010	0.015
Σ _{oct. and VIII}	1.991	1.982	1.992	2.025	1.990	2.008	1.989	2.017	1.994
Σ _{cations}	3.991	3.980	3.987	4.005	3.987	3.999	3.989	4.001	3.994
Wo	38.4	7.3	36.5	11.0	36.3	4.3	25.3	11.1	18.6
En	44.9	62.4	41.0	61.4	40.7	74.9	41.1	56.4	26.8
Fs	16.7	30.3	22.5	27.6	23.0	20.8	33.6	32.5	54.6

* All analyses normalized to six oxygens; Columns (1-2): anorthositic gabbro; Columns (3-4): norite; Column (5): light matrix breccia; Columns (6-7): recrystallized noritic breccia; Columns (8-9): feldspathic basalt.

(5) Very Low Ti (VLT) Basalt

This basalt type is described in detail by Vaniman and Papike (1977a,b) and Taylor et al. (1977). The VLT basalt is subophitic, with abundant pyroxene (~ 60 modal %) enclosing euhedral spinel (Fig 2f). The low Ti content (< 0.5 wt.%) of VLT basalt is reflected in the low initial Ti/Al ratios in pyroxene (Fig. 5) and in the occurrence of CrAl spinel as the primary oxide phase with ilmenite and ulvöspinel as residual phases. For a more complete description see Vaniman and Papike (1977b).

Vitrophyres of the VLT basalt-type contain spinel and olivine (Fo₇₅) as near-liquidus phases. Olivine in phaneritic VLT is zoned to Fo₅₅. The pyroxenes of phaneritic VLT basalt have extreme Fe-enrichment trends (Fig. 3). The low initial Ti/Al zoning trend of pyroxene (Fig. 5) reverses and rises toward Ti:Al = 1:2; this reversal records the first appearance of plagioclase in the VLT crystallization sequence. A reversal due to plagioclase precipitation is also seen in Ca enrichment of the (110) pyroxene sectors (Fig. 3). The initial Ti:Al ratio in VLT pyroxene zonation is much lower than the Ti:Al ratio of pyroxenes in any other lithic component, mare or highland, in the Apollo 17 drill core (Fig. 5). This typically low Ti content distinguishes VLT pyroxenes in the monomineralic component.

THE HIGHLAND LITHIC COMPONENT

The original highland sample descriptions of LSPET (1973) emphasized two highland lithic types: a friable anorthositic gabbro with plagioclase cumulate texture, and a "hornfelsic" (i.e., tough, interlocking crystalline) KREEP-rich noritic breccia. Rhodes et al. (1974) related the

North Massif-Sculptured Hills highlands with anorthositic gabbro and the South Massif highlands with equal amounts of norite and anorthositic gabbro. These authors suggested that lateral transport at the landing site has been minimal, and they showed that the surface soils have a highland component that reflects the composition of the closest massif. The drill-core site is equidistant from the North Massif and from the light-mantle landslide soils of the South Massif and, therefore, should have a mixed highland component that is dominantly anorthositic gabbro. Hawke and Ehmann (1976) used mixing-models to derive anorthositic gabbro/norite ratios of $\sim 1:1$ for South Massif, $\sim 2:1$ for North Massif-Sculptured Hills, and $\sim 7:6$ for the drill site. Thus, the work of both Rhodes et al. (1974) and Hawke and Ehmann (1976) suggests that anorthositic gabbro is an important highland component in the drill core.

These soil models are based on chemical data. The petrographic data from the 2-4 mm surface soils show no anorthositic gabbro in the dark soils of the Taurus-Littrow Valley (Stations 1a, 5, 9: ref. Bence et al., 1974). However, modal data (Table 1a) show that noritic fragments are twice as abundant as anorthositic gabbro in the > 0.02 mm soil fraction of 70007, whereas in the upper core (70008 and 70009) anorthositic fragments are as abundant as noritic fragments. In general the soil models of Rhodes et al. (1974) and Hawke and Ehmann (1976) hold true within the upper drill core.

The noritic, anorthositic gabbro, and "other" highland lithic types which have been recognized in the drill core are described below. Mineral data for each rock type are summarized in Tables 3, 5, 7 and 8 and in Figs. 4, 6, 8 and 9.

Table 4

Olivine Compositions* : Mare Component

	1	2	3	4	5	6	7	8
SiO ₂	37.90	38.07	37.66	36.94	36.75	35.56	37.34	37.98
Al ₂ O ₃	0.11	0.17	0.00	0.00	0.00	0.25	0.14	0.18
TiO ₂	0.38	0.39	0.18	0.23	0.16	0.46	0.05	0.07
FeO	23.65	21.45	24.43	28.34	31.77	37.69	28.79	23.06
MnO	0.27	0.20	0.18	0.31	0.29	0.39	0.31	0.29
MgO	37.84	39.57	37.70	33.78	31.96	26.24	33.85	37.94
CaO	0.46	0.40	0.29	0.38	0.29	0.24	0.24	0.41
Cr ₂ O ₃	0.37	0.50	0.23	0.17	0.15	0.11	0.39	0.55
Total:	100.98	100.75	100.67	100.15	101.37	100.94	101.11	100.48
Si	0.985	0.982	0.985	0.991	0.991	0.991	0.992	0.989
Al	0.004	0.005	0.000	0.000	0.000	0.008	0.004	0.006
Ti	0.007	0.008	0.003	0.005	0.003	0.010	0.001	0.001
Fe	0.514	0.463	0.534	0.636	0.713	0.878	0.640	0.502
Mn	0.006	0.004	0.004	0.007	0.007	0.009	0.007	0.006
Mg	1.466	1.521	1.469	1.350	1.279	1.090	1.341	1.473
Ca	0.013	0.011	0.008	0.011	0.008	0.007	0.007	0.012
Cr	0.008	0.010	0.005	0.004	0.003	0.002	0.008	0.011
Σ cations	3.003	3.004	3.008	3.004	3.004	2.995	3.000	3.000
Fo	73.8	76.5	73.2	67.8	64.0	55.1	65.2	74.3
Fa	26.2	23.5	26.8	32.2	36.0	44.9	34.8	25.7

* All analyses normalized to four oxygens; Columns (1-2): Olivine porphyritic ilmenite basalt; Columns (3-4): Intermediate texture ilmenite basalt; Column (5): Plagioclase poikilitic ilmenite basalt; Column (6): Diabasic/ophitic ilmenite basalt; Column (7): Very low-Ti (VLT) basalt; Column (8): Very low-Ti (VLT) basalt vitrophyre.

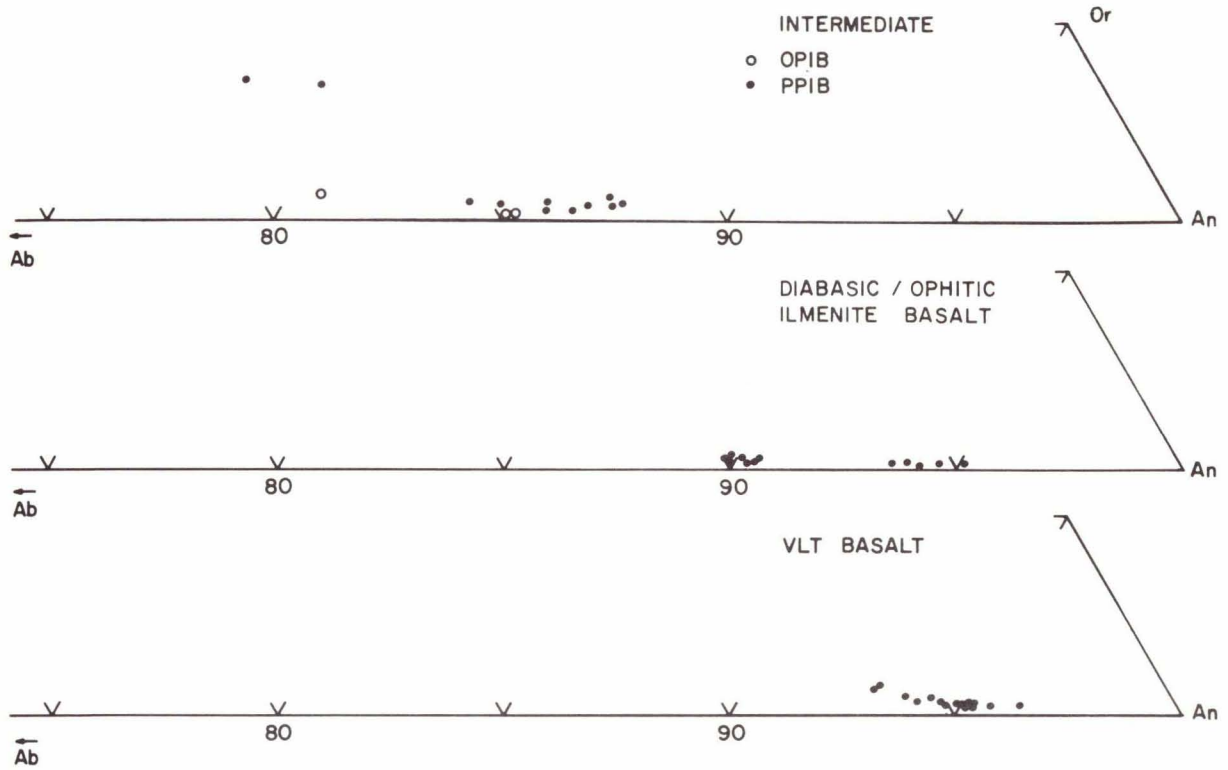
Table 5

Olivine Compositions* : Highland Component						
	1	2	3	4	5	6
SiO ₂	36.64	38.44	40.41	37.38	40.01	39.18
Al ₂ O ₃	0.17	0.00	0.00	0.00	0.00	0.18
TiO ₂	0.14	0.00	0.06	0.10	0.16	0.15
FeO	32.45	22.79	12.55	29.13	13.64	19.80
MnO	0.27	0.21	0.10	0.23	0.13	0.19
MgO	31.55	38.62	47.82	33.46	46.93	41.39
CaO	0.20	0.43	0.11	0.35	0.19	0.29
Cr ₂ O ₃	0.07	0.44	0.00	0.04	0.14	0.08
Total	101.49	100.93	101.05	100.69	101.20	101.26
Si	0.987	0.994	0.992	0.998	0.987	0.994
Al	0.005	0.000	0.000	0.000	0.000	0.005
Ti	0.003	0.000	0.001	0.002	0.003	0.003
Fe	0.731	0.493	0.258	0.651	0.282	0.420
Mn	0.006	0.004	0.002	0.005	0.003	0.004
Mg	1.267	1.489	1.750	1.332	1.726	1.565
Ca	0.006	0.012	0.003	0.010	0.005	0.008
Cr	0.001	0.009	0.000	0.001	0.003	0.002
Σ cations	3.006	3.001	3.006	2.999	3.009	3.001
Fo	63.2	75.0	87.1	67.0	85.9	78.7
Fa	36.8	25.0	12.9	33.0	14.1	21.3

* All analyses normalized to four oxygens; Column (1): Anorthositic gabbro; Columns (2-3): Norite; Columns (4-5): Recrystallized noritic breccias; Column (6): Feldspathic basalt.

FELDSPAR

Mare Lithic Component



Highland Lithic Component

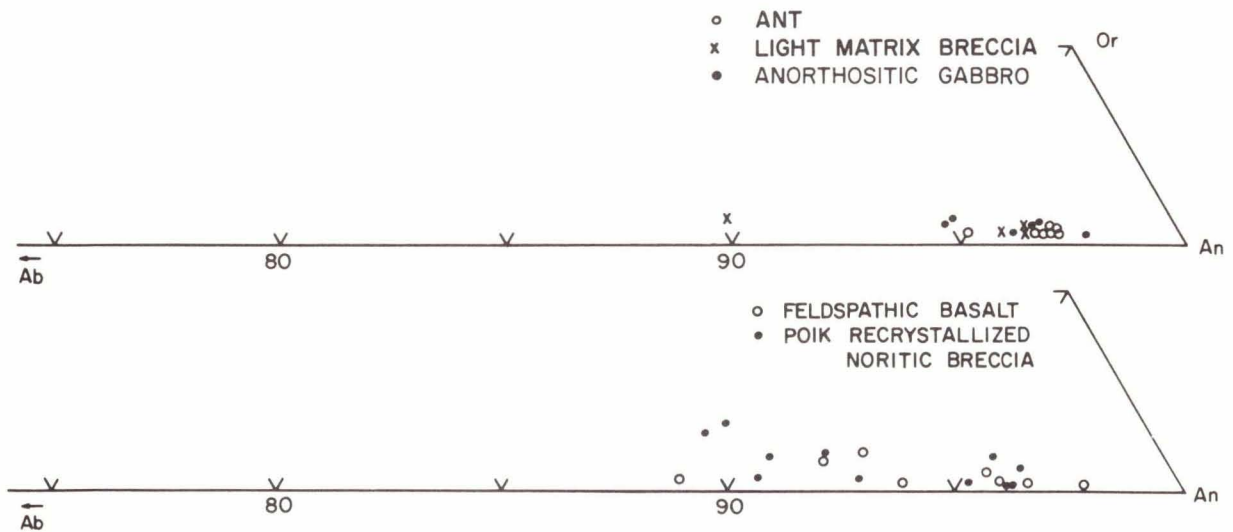


Fig. 9. Ab-An-Or feldspar compositions in mare and highland lithics.

Table 6

Feldspar Compositions*: Mare Component

	1	2	3	4	5	6	7
SiO ₂	47.41	45.82	48.20	50.35	47.27	47.61	46.17
Al ₂ O ₃	33.23	34.43	32.62	30.62	33.66	32.97	33.72
FeO	1.19	0.75	0.79	0.98	0.48	0.47	0.98
MgO	0.16	0.00	0.18	0.02	0.17	0.21	0.18
CaO	18.26	18.16	16.85	14.51	17.53	17.48	19.08
Na ₂ O	1.11	1.03	1.62	2.40	1.48	1.52	0.54
K ₂ O	0.04	0.12	0.03	0.58	0.06	0.04	0.04
Total:	101.40	100.31	100.29	99.46	100.65	100.30	100.71
Si	2.161	2.110	2.208	2.316	2.161	2.183	2.122
Al	1.786	1.870	1.761	1.660	1.814	1.782	1.828
Σ	3.947	3.980	3.969	3.976	3.975	3.965	3.950
Fe	0.045	0.029	0.030	0.038	0.018	0.018	0.038
Mg	0.011	0.000	0.012	0.001	0.012	0.015	0.012
Ca	0.892	0.896	0.827	0.715	0.859	0.859	0.940
Na	0.098	0.092	0.144	0.214	0.131	0.135	0.048
K	0.002	0.007	0.002	0.034	0.004	0.003	0.002
Σ	1.048	1.024	1.015	1.002	1.024	1.030	1.040
Σ _{cations}	4.995	5.004	4.984	4.978	4.999	4.995	4.990
Or	0.2	0.7	0.2	3.6	0.4	0.2	0.2
Ab	9.9	9.2	14.8	22.2	13.2	13.6	4.8
An	89.9	90.1	85.0	74.2	86.4	86.2	95.0
Fe/(Fe + Mg)	0.80	1.00	0.71	0.96	0.61	0.55	0.75

* All analyses normalized to eight oxygens; Columns (1-2): High-Ti vitrophyres; Column (3): olivine porphyritic high-Ti basalt; Columns (4-6): plagioclase poikilitic high-Ti basalt; Column (7): very low-Ti (VLT) basalt.

Table 7

Feldspar Compositions* : Highland Component

	1	2	3	4	5	6	7	8	9	T0
SiO ₂	44.32	44.71	44.73	44.60	44.97	43.80	50.94	44.08	45.40	44.50
Al ₂ O ₃	35.98	35.36	34.44	34.95	34.68	36.52	31.07	36.41	35.45	35.80
FeO	0.24	0.23	0.28	0.20	0.30	0.19	0.46	0.23	0.42	0.37
MgO	0.00	0.00	0.02	0.01	0.00	0.00	0.16	0.00	0.00	0.02
CaO	19.20	19.37	19.25	19.38	17.80	19.80	14.54	19.66	18.63	19.85
Na ₂ O	0.54	0.44	0.55	0.36	1.06	0.31	2.78	0.38	0.84	0.24
K ₂ O	0.09	0.08	0.04	0.05	0.11	0.05	0.38	0.08	0.13	0.01
Total:	100.37	100.19	99.31	99.55	98.92	100.67	100.33	100.84	100.87	100.79
Si	2.042	2.063	2.083	2.070	2.095	2.015	2.316	2.024	2.079	2.044
Al	1.955	1.924	1.891	1.913	1.906	1.981	1.666	1.971	1.914	1.939
Σ	3.997	3.987	3.974	3.983	4.001	3.996	3.982	3.995	3.993	3.983
Fe	0.009	0.009	0.011	0.008	0.012	0.007	0.017	0.009	0.016	0.014
Mg	0.000	0.000	0.002	0.001	0.000	0.000	0.011	0.000	0.000	0.001
Ca	0.948	0.958	0.960	0.964	0.889	0.976	0.708	0.968	0.914	0.977
Na	0.048	0.039	0.049	0.032	0.096	0.028	0.245	0.033	0.075	0.021
K	0.006	0.005	0.002	0.003	0.006	0.003	0.021	0.005	0.008	0.001
Σ	1.011	1.011	1.024	1.008	1.003	1.014	1.002	1.015	1.013	1.014
Σ _{cations}	5.008	4.998	4.998	4.991	5.004	5.010	4.984	5.010	5.006	4.997
Or	0.6	0.5	0.2	0.3	0.6	0.3	2.3	0.5	0.8	0.1
Ab	4.8	3.9	4.9	3.2	9.7	2.8	25.1	3.3	7.5	2.1
An	94.6	95.6	94.9	96.5	89.7	96.9	72.6	96.2	91.7	97.8
Fe/(Fe + Mg)	1.00	1.00	0.87	0.94	1.00	1.00	0.61	1.00	1.00	0.93

* All analyses normalized to eight oxygens; Columns (1-2): Anorthositic gabbro; Columns (3-4): Norite; Column (5-6): Light-matrix breccia; Columns (7-8): Recrystallized noritic breccia; Columns (9-10): Feldspathic basalt.

KREEP-Rich Noritic Breccia (and Textural Variants)

The KREEP-rich norites constitute an approximately isochemical series that ranges from metamorphic textured rocks to melt rocks (Bence et al., 1974). In order of increasing melt features these are:

(a) Recrystallized Noritic Breccia (RNB)

This rock type is characterized by subequant beads of pyroxene and olivine between clasts of feldspar and lithic fragments (Fig. 2i). Clasts and matrix tend to be poorly equilibrated, though highly recrystallized fragments with triple-junction grain boundaries approach intergrain chemical equilibration (Bence et al., 1974). The name "norite" is justified by an abundant low-Ca pyroxene component ($Wo_5En_{73}Fs_{22}$) with lesser amounts of diopsidic augite and olivine ($\sim Fo_{75}$). Bence et al. (1974) interpret the RNB texture as essentially metamorphic.

(b) Pyroxene Poikilitic Rocks (POIK Rocks)

POIK rocks have low-Ca pyroxene (\pm high-Ca pyroxene, olivine) in poikilitic growth around smaller feldspar grains (Fig. 2g). The pyroxene may be pigeonite, indicating high-temperature equilibration within a clast-laden melt (Simonds et al., 1973; Irving, 1975), or an equilibrated lower temperature pyroxene pair suggesting metamorphism (Bence et al., 1973; Ridley and Adams, 1976). The ranges of pyroxene, olivine, and feldspar compositions of RNB and POIK lithics within the drill core overlap, and we have plotted these two lithic types as a single group (Figs. 4, 6, 8).

(c) Feldspathic Basalt

The feldspathic basalts of the Apollo 17 core are diabasic in texture, intergranular to intersertal, with abundant feldspar (\sim 50-60%) and intergranular crystals of low-Ca to intermediate-Ca pyroxene, olivine

and ilmenite (Fig. 2h). The pyroxenes of feldspathic basalt may be more iron-rich than those of the RNB and POIK rocks. The feldspathic basalts are chemically equivalent to the other Apollo 17 noritic rock types; all of these rocks plot near the olivine-plagioclase-pyroxene peritectic of the SiO_2 -olivine-anorthite pseudoternary diagram (Bence et al., 1974). However, textural evidence for earliest precipitation of feldspar in the intersertal varieties indicates that the feldspathic basalts are significantly more An-rich than the olivine-plagioclase-pyroxene peritectic composition.

Some of the diabasic-textured melt rocks found by Bence et al. (1974) in the 2-4 mm surface soils have not been recognized in the drill core. These include spinel-bearing rocks with large (0.5 mm) feldspar clasts in a fine diabasic matrix and KREEP-rich melt rocks with K-feldspar in residual veins.

Anorthositic Gabbros

"Anorthositic gabbro" is a rock name tied to a specific highland composition ($\text{Al}_2\text{O}_3 \sim 26\%$, $\text{FeO} \sim 6\%$, $\text{MgO} \sim 6\%$, $\text{CaO} \sim 15\%$; with normative An $\sim 70\%$, Px $\sim 14\%$, Ol $\sim 10\%$; LSPET, 1973). The type-lithic for this composition is 77017, a feldspar cumulate rock which entrapped much of the parental magma's residual liquid (McCallum et al., 1974; Schonfeld, 1975). Bence et al. (1974) preferred the term "gabbroic anorthosite" for this rock type, because of its feldspar-rich normative composition. In this paper the original term anorthositic gabbro will be retained because of its chemical significance in highland petrology.

Anorthositic gabbros of the Apollo 17 drill core have distinctive feldspar grains enclosing beads or "necklaces" of olivine; the feldspars

Table 8

Oxide Compositions* : Mare and Highland Components

	1	2	3	4	5	6	7	8	9
Al ₂ O ₃	15.83	0.00	1.89	0.17	0.00	0.00	16.96	6.09	0.00
TiO ₂	9.77	52.39	74.99	51.61	52.56	54.09	0.89	16.91	54.84
FeO	27.84	44.48	14.64	44.80	45.85	41.63	28.29	47.55	39.62
MnO	0.34	0.47	0.07	0.37	0.40	0.35	0.35	0.32	0.34
MgO	9.54	0.71	7.53	1.48	0.48	3.31	5.19	1.48	5.40
Cr ₂ O ₃	37.32	0.30	2.06	0.72	0.16	0.59	49.24	28.41	0.64
Total	100.64	98.35	101.18	99.15	99.45	99.97	100.92	100.76	100.84
Al	0.598	0.000	0.078	0.005	0.000	0.000	0.658	0.255	0.000
Ti	0.236	1.003	1.985	0.981	1.000	1.000	0.022	0.451	0.992
Fe	0.747	0.947	0.431	0.946	0.970	0.855	0.780	1.410	0.797
Mn	0.009	0.010	0.002	0.008	0.009	0.007	0.010	0.010	0.007
Mg	0.456	0.027	0.395	0.056	0.018	0.121	0.254	0.078	0.193
Cr	0.946	0.006	0.058	0.013	0.003	0.011	1.283	0.797	0.012
Σ cations	2.992	1.993	2.949	2.009	2.000	1.994	3.007	3.001	2.001
Fe/(Fe + Mg)	0.621	0.972	0.522	0.944	0.982	0.876	0.754	0.948	0.805
(Cr/2):(Al/2):Ti	47:30:23	---	---	---	---	---	65:33:02	13:41:46	---
Al/Cr	0.632	---	1.345	---	---	---	0.513	0.320	---

* Armalcolite normalized to five oxygens, ilmenites normalized to three oxygens, spinels normalized to four oxygens; Column (1): Spinel, olivine porphyritic ilmenite basalt; Column (2): Ilmenite, olivine porphyritic ilmenite basalt; Column (3): Armalcolite, olivine porphyritic ilmenite basalt; Column (4): Ilmenite, olivine porphyritic ilmenite basalt; Columns (5-6): Ilmenites, plagioclase poikilitic ilmenite basalt; Column (7): Spinel, very low-Ti (VLT) basalt; Column (8): Spinel, very low-Ti (VLT) vitrophyre; Column (9): Ilmenite, recrystallized noritic breccia.

themselves are surrounded by a mortar-like matrix of poikilitic Ca-poor and Ca-rich pyroxene (Fig. 2j). These rocks are highly equilibrated, with a distinctive low-Ca pyroxene component ($\sim \text{Wo}_8\text{En}_{65}\text{Fs}_{27}$) and olivines (Fo_{60-70}) which are more Fe-rich than the POIK/RNB olivines (Fig. 4).

Other Highland Lithologies

Other highland lithologies in the drill core are rare. However, the proposal of Arvidson et al. (1976) that the Central Cluster craters are due to Tycho ejecta raises the possibility that some of this material could be exotic (Delano, 1977).

(a) Anorthosites

Fragments of coarse-grained highland anorthosite (> 90% plag.) would have to be exceptionally large (several millimeters) to be recognized as polycrystalline fragments in the drill core. Such fragments have not been found, though single crystals from coarse anorthosite may be present among the monomineralic plagioclase fragments of An_{95-98} . We have classified as "anorthosite" those polycrystalline plagioclase fragments with recrystallized or melt-rock (diabasic) textures, and plagioclase of $\sim \text{An}_{95}$.

(b) Light Matrix Breccias (LMB)

Light matrix breccias are unequilibrated anorthositic breccias with clear-to-yellow glass in their matrix (Fig. 2k; Delano et al., 1973; and Warner et al., 1973). A broad size range of crushed feldspar grains (~ 1 mm to < 0.02 mm) is characteristic, with $< 5\%$ pyroxene and olivine and $\sim 5-30\%$ glass. Opaque phases consist of intergrain Fe-metal and ilmenite. In recent work Warner et al. (1977) have suggested the term "vitric matrix breccia" for such rocks. Simonds et al. (1976) classify this rock type as "fragmental-matrix polymict breccia" to distinguish it from other impact breccias which are dominantly glassy.

(c) *Recrystallized Peridotite*

PTS 70008,354 contains one fragment of recrystallized peridotite (20% $Wo_3En_{87}Fs_{10}$; ~ 10% $Wo_{48}En_{49}Fs_3$; ~ 60% Fo_{87} ; ~ 10% An_{97}). This fragment is shown in Fig. 2. Pyroxene compositions indicate re-equilibration to very low temperature, but a bimodal distribution of grain size is retained. No pyroxene fragments characteristic of this Mg-rich rock have been found in the monomineralic population, although single olivine crystals of Mg content Fo_{81} or greater are common in core section 70007 (Fig. 13).

THE MONOMINERALIC COMPONENT

All single crystals of pyroxene, feldspar and olivine were analyzed in selected areas of four thin sections. These data are summarized in Figs. 10-12 for comparison with the mineral systematics of possible lithic sources. The relationship of these four areas to the modal stratigraphy of Papike et al. (1977) is shown in Fig. 1: 70009,288 is above the coarse-grained unit; 70008,356 is within the coarse-grained unit; 70007,312 is at the base of the coarse-grained unit; and 70007,332 is below the coarse-grained unit. The monomineralic fragments within these four areas are more abundant than the lithic fragments and thus provide much of the data for determining stratigraphic variations and provenance. Each mineral type provides distinctive information.

Pyroxene Grains

The Wo-En-Fs "quad" compositions of pyroxenes (Fig. 10) show considerable Fe-enrichment above the coarse-grained unit. This is the trend corresponding to the equilibrated PPIB high-Ti basalts. The

MONOMINERALIC PYROXENE AND OLIVINE

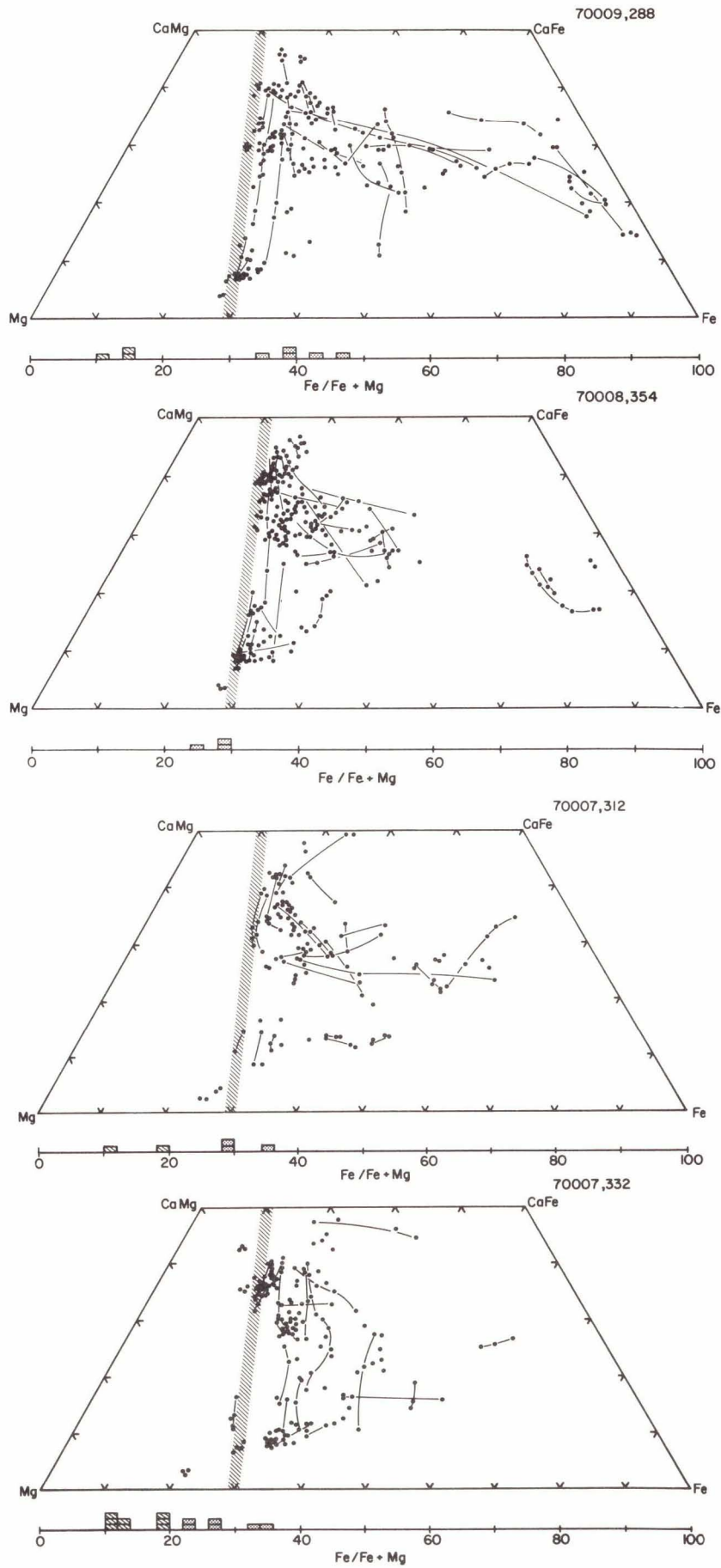


Fig. 10. Stratigraphy of Ca-Fe-Mg pyroxene composition and Fe-Mg olivine composition in core segments 70009, 70008 and 70007.

pyroxene Ti contents (< 0.12 atoms/6 oxygens) and Al contents (< 0.25 atoms/6 ox.), with Ti:Al ratios of 1:2, are also typical of PPIB basalt. Moreover, the pyroxene Al/Si ratios are low (< 0.1), as in PPIB.

Within the coarse-grained unit (PTS 70008,354) the major element "quad" compositions of pyroxene grains are dominated by the Ca-depletion trend of "intermediate" high-Ti basalt. The Al + Ti contents (up to 0.4 Al/6 ox. and 0.2 Ti/6 ox.) reflect "intermediate" basalt pyroxene types. Pyroxene grains in this unit also have Al/Si ratios of 0.2-0.3 characteristic of "intermediate" basalt types.

PTS 70007,312 is at the very base of the coarse-grained unit and appears to be transitional into the lower unit. PTS 70007,332 is well below the coarse-grained unit and is quite distinctive. Stippled bars in the "quad" diagrams (Fig. 10) show the approximate Mg-rich limit of Apollo 17 mare pyroxene compositions, and pyroxenes more Mg-rich than this limit are found only in PTS 70007,332. This is a further indication of the increased highland component below the coarse layer.

Mare pyroxenes in 70007,332 differ from mare pyroxenes higher in the core. Figure 11 shows very high Ti and Al content in these pyroxenes (up to 0.5 Al/6 ox. and 0.15 Ti/6 ox.), and a significant drop below the Ti/Al ratio 1:2 at high Ti + Al contents. These features are characteristic of OPIB. High Al/Si ratios (~ 0.4 ; Fig. 12) at high values of Fe/(Fe + Mg) are also characteristic of OPIB pyroxene.

It should be noted that pyroxenes with low Ti/Al ratios ($< 1/2$) and low Ti and Al content (Ti < 0.01 atoms/6 ox., Al < 0.05 atoms/6 ox.) appear in several of the four thin sections analyzed. These may be highland pyroxenes, but if so they are unlike those from the highland lithics within the core (Fig. 6). VLT basalts are a more likely source for pyroxenes with these low Ti/Al ratios.

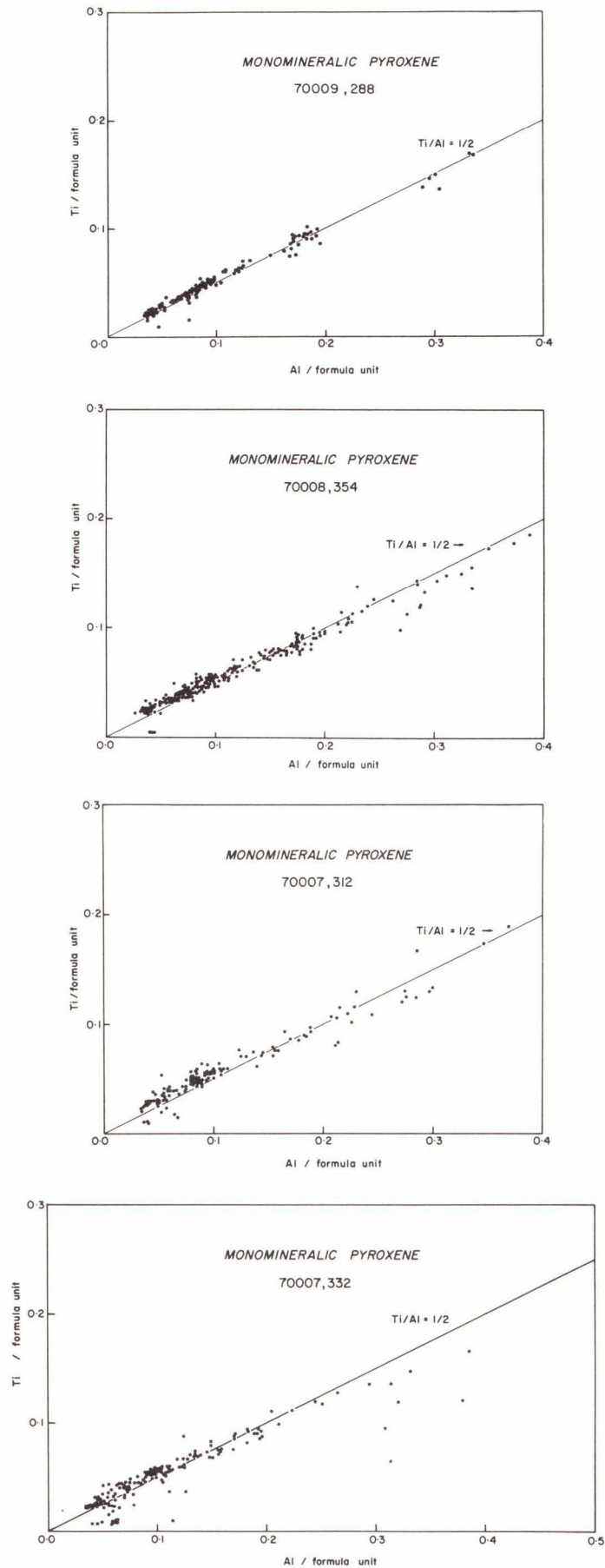


Fig. 11. Stratigraphy of pyroxene Ti vs Al content (atoms per 6-oxygen formula unit) in core segments 70009, 70008 and 70007.

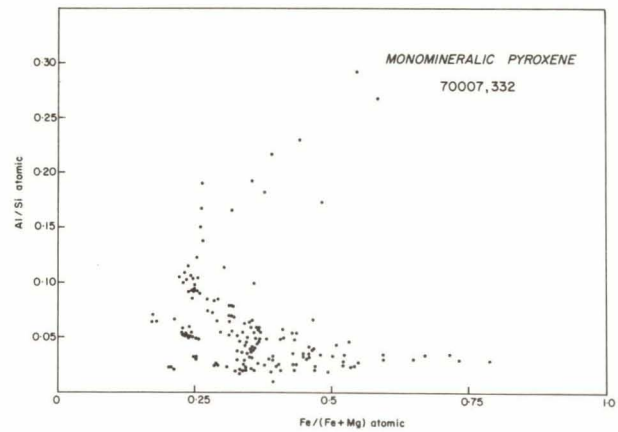
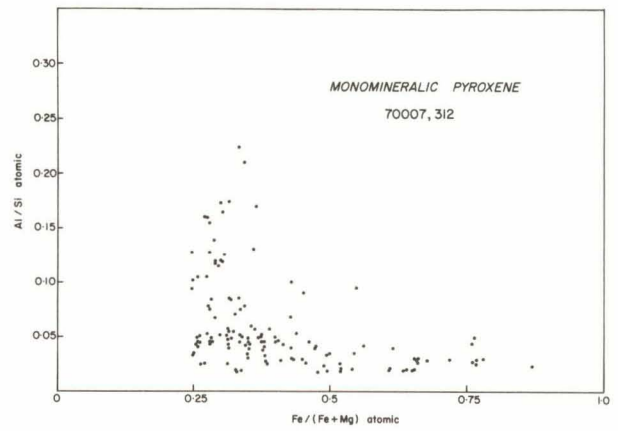
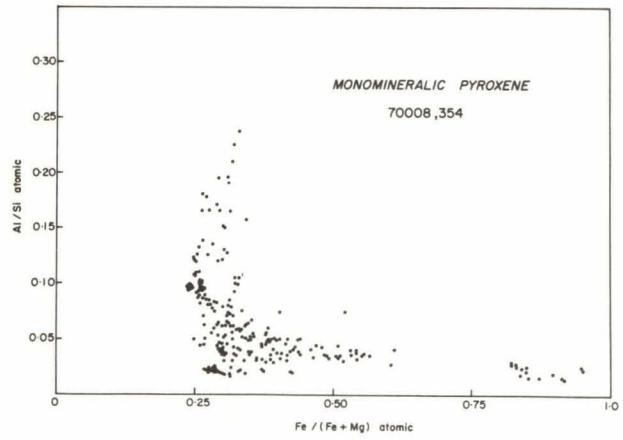
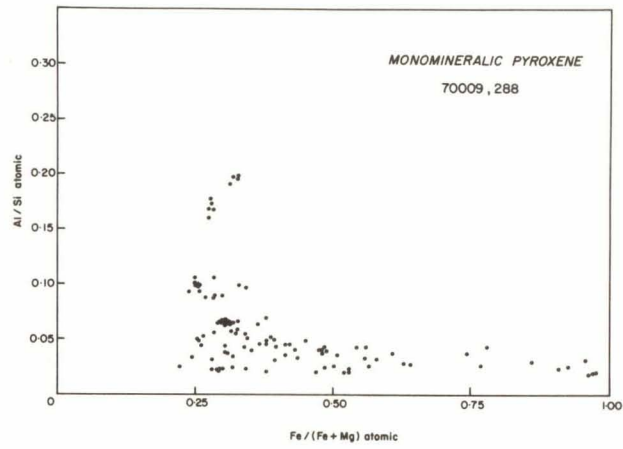


Fig. 12. Stratigraphy of pyroxene Al/Si vs Fe/(Fe + Mg) (atomic ratios) in core segments 70009, 70008 and 70007.

Olivine Grains

Mg-Fe contents of olivine grains are summarized in Fig. 13. An important breakpoint in the olivine compositions of the drill core is $\sim \text{Fo}_{78}$, for this is the most magnesian olivine of mare basalts in the Taurus-Littrow Valley (Papike *et al.*, 1976). More magnesian olivines (Fo_{78-90}) are found in 70009,288, and 70007,332 above and below the coarse unit, but are absent within the coarse-grained unit (70008,354) and rare at the base of this unit (70007,312). The greatest abundance of high-Mg olivine is in PTS 70007,332, marking a greatly increased highland component below the coarse-grained unit. This increased Mg-rich olivine content is the most abundant single indicator of the highland component in 70007. Thus, the dominant source of highland material found below the coarse unit must be olivine-rich.

Feldspar Grains

Feldspars more calcic than An_{90} are more abundant above and below the coarse-grained layer (Fig. 14). Certainly, some (if not all) of this calcic plagioclase is part of the highland component that is also indicated by Mg-rich olivine above and below the coarse-grained unit. However, VLT basalt and diabasic/ophitic ilmenite basalt also have feldspar in this compositional range, and these lithic types may contribute to the high-Ca plagioclase component above and below the coarse unit.

The modal abundances of plagioclase fragments are a significant clue to the nature of the highland component. In a companion paper, Papike and Vaniman (1977c) show that the coarse unit (x-ray unit 59) has more plagioclase than the units above and below. However, Ali and Ehmann (1977) have shown a plagioclase enrichment (Ca, Al increase) below the coarse unit in 70007. This plagioclase-rich component must be in the

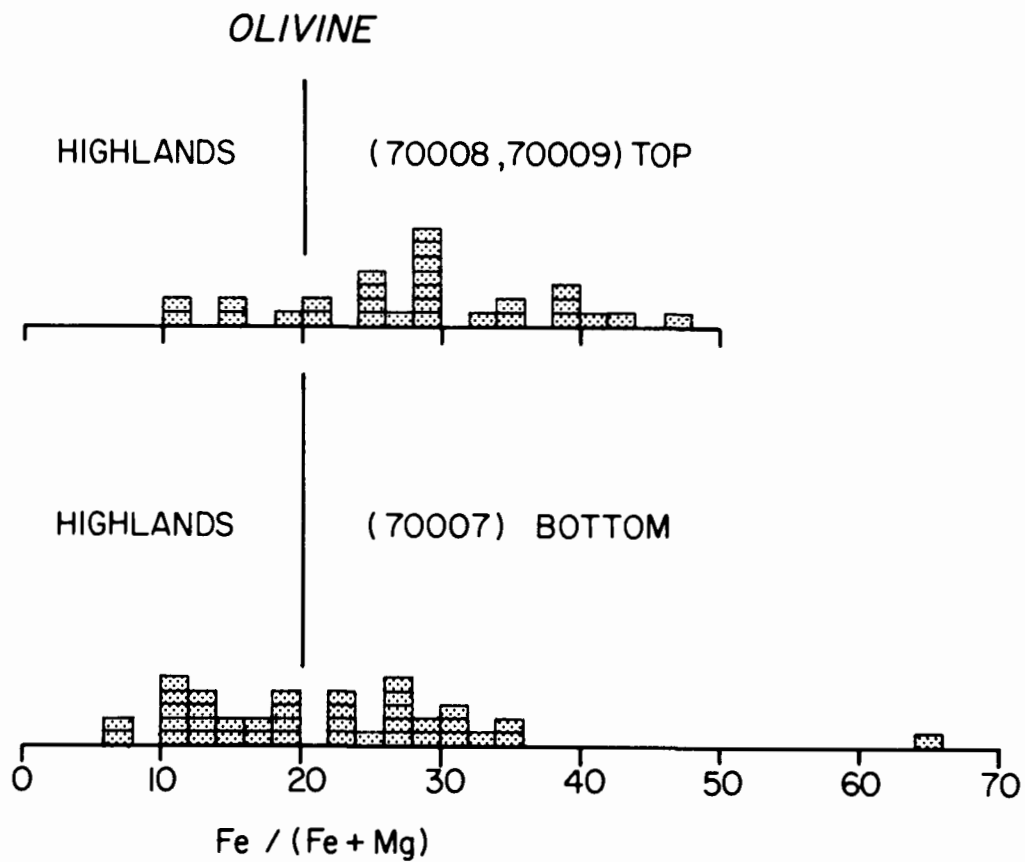


Fig. 13. Atomic $Fe/(Fe + Mg)$ ratio in olivine fragments: comparison between the bottom of core segment 70007 (PTS 70007,332) and the upper core segments 70009 and 70008. Olivines more Mg-rich than Fa_{20} are derived from highland sources.

MONOMINERALIC FELDSPAR

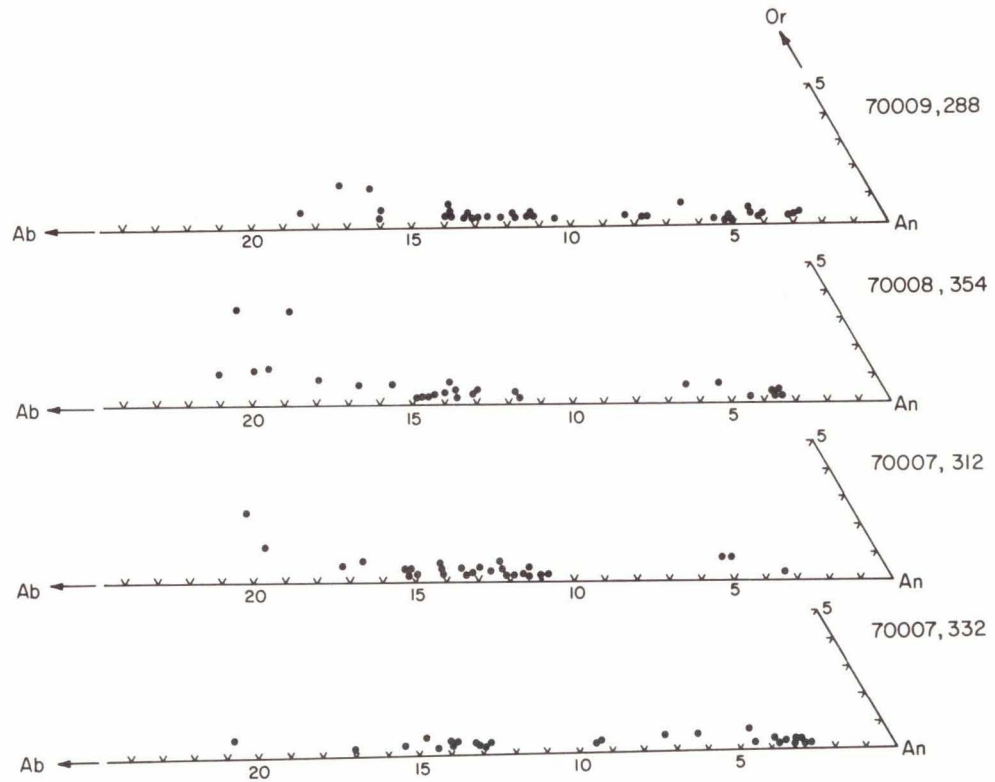


Fig. 14 Stratigraphy of Ab-An-Or feldspar compositions in core segments 70009, 70008 and 70007.

< 0.02 mm size fraction (\sim 65% of the soils) which could not be characterized in modal analysis. Nevertheless, it is surprising that the highland component, which can be seen below the coarse unit in the > 0.02 mm pyroxene component and both above and below the coarse unit in the > 0.02 mm olivine component, is not marked by a more pronounced increase in plagioclase > 0.02 mm. This may in part be due to the increase of feldspar-poor OPIB as a soil component below the coarse unit, but in addition to this effect the principal sources of the monomineralic highland component must have been relatively mafic, and not plagioclase-rich anorthosites.

CONCLUSIONS

Data on the stratigraphy of mineral and lithic fragments in the Apollo 17 drill core lead to the following conclusions:

(1) The dominant highland component in the upper Apollo 17 drill core (sections 70007, 70008, 70009) was mafic. The characteristic mineralogy of this source included Mg-rich olivine (\sim Fo₈₀₋₉₀), low-Ca and high-Ca pyroxene, and calcic feldspar (\sim An₉₅). There are no lithic fragments of this component within the core, but Bence et al. (1974) describe 2-4 mm POIK fragments with this mineralogy as the only significant highland component of the dark soils near the drill site.

(2) The highland component increases below the coarse-grained unit, and is somewhat enriched above the coarse unit. The coarse unit itself is composed almost entirely of mare-derived lithic and mineral fragments.

(3) Monomineralic pyroxenes reveal a stratigraphy of high-Ti basalt types within the drill core:

(a) PPIB and "intermediate" basalt predominate above and within the coarse unit,

(b) OPIB becomes more abundant below the coarse unit.

LSPET (1973) have suggested that the coarse unit may be an overturned ejecta flap from Camelot Crater, ~ 1 crater diameter distant from the drill site. If this is so, the nearest overlying and underlying units (70009 and 70007) may be part of this flap. Therefore, the basalt sequence outlined above could be a cross section of a single subfloor basalt flow excavated by the Camelot impact: the chilled upper contact of that flow is now overturned and is below the coarse layer in the drill core. The deeper, more fractionated parts of the flow unit contain PPIB and occur at the top of the overturned flap in the drill (70008, 70009). Re-excavation and refilling of 70009 ~ 2 m.y. ago (Fruchter et al., 1976) may have only reshuffled the soils in 70009 without significantly altering the nature of the basaltic component. Taylor et al. (1977) have suggested that the soils in 70007 may be derived from smaller craters of the Central Cluster (e.g., San Luis Rey) which are farther from the drill site than Camelot Crater. If this is the case, the OPIB basalts in 70007 would not represent the chilled upper contact of the basalts in 70008; nevertheless, these OPIB fragments would be from smaller craters that must have sampled shallower parts of the subfloor basalt than were sampled by Camelot Crater. Whether the OPIB fragments of 70007 come from Camelot or the Central Cluster, the inversion of a subfloor basalt sequence in 70009, 70008, 70007 seems quite possible.

(4) The OPIB-PPIB basalts of the Apollo 17 drill core show a broader spectrum of fractionation than the large basalt fragments which

have been sampled at the landing site. Fe-enrichment is much more pronounced in basalts of the drill core (Figs. 3, 10) than in basalts of the 2-4 mm surface component, including material from the rim of Camelot Crater (Papike et al., 1974). The broad spectrum of OPIB-PPIB basalt variation in the drill core is due to the large population and stratigraphic variation of basalt fragments within the core. These fragments of very high-Ti basalt within the drill core may provide the only Apollo 17 sample which is an almost complete and nearly intact section into one of the subfloor Taurus-Littrow basalts.

ACKNOWLEDGMENTS

We acknowledge Dr. A. Basu and Dr. D. Lindstrom for careful review and suggestions.

This research was funded by NASA Grant #NSG-9044, which we gratefully acknowledge.

REFERENCES

- Albee A. L. and Ray L. (1970) Correction factors for electron probe microanalysis of silicates, oxides, carbonates, phosphates and sulfates. Anal. Chem., 42, 1408-1414.
- Ali M. Z. and Ehmann W. D. (1977a) Chemical characterization of Apollo 17 deep drill cores 70007-70009. Lunar Sci. VIII, 13-15.
- Arvidson R., Drozd R., Guinness E., Hohenberg C., Morgan C., Morrison R., and Oberbeck V. (1976) Cosmic ray exposure ages of Apollo 17 samples and the age of Tycho. Proc. Lunar Sci. Conf. 7th, 2817-2832.
- Bence A. E. and Albee A. L. (1968) Empirical correction factors for electron microanalysis of silicates and oxides. Jour. Geology, 76, 382-403.
- Bence A.E., Delano J. W., Papike J. J. and Cameron K. L. (1974) Petrology of the highlands massifs at Taurus-Littrow: An analysis of the 2-4 mm soil fraction. Proc. Lunar Sci. Conf. 5th, 785-827.
- Brown G. M., Peckett A., Emelous C. H., Phillips R., and Pinsent R. H. (1975) Petrology and mineralogy of Apollo 17 mare basalts. Proc. Lunar Sci. Conf. 6th, 1-13.
- Crozaz G. and Plachy A. L. (1976) Origin of the Apollo 17 deep drill coarse-grained layer. Proc. Lunar Sci. Conf. 7th, 123-131.
- Curtis D. and Wasserburg G. J. (1975) Apollo 17 neutron stratigraphy-sedimentation and mixing in the lunar regolith. The Moon, 13, 185-227.

- Delano J. W., Bence A. E., Papike J. J. and Cameron K. L. (1973)
Petrology of the 2-4 mm soil fraction from the Descartes region
of the moon and stratigraphic implications. Proc. Lunar Sci.
Conf. 4th, 537-551.
- Delano J. W. (1977) The highlands component in the Apollo 17 soils.
Lunar Sci. VIII, 236-238.
- Duke M. B. and Nagle J. S. (1974) Lunar Core Catalog, NASA publication
JSC 09252. 242 pp.
- El Goresy A. and Ramdohr P. (1977) Apollo 17 TiO₂-rich basalts: Spinel
chemical bimodality in the two major basalt types and genetic
significance of inverted zoning of chromian ulvöspinel. Lunar
Sci. VIII, 281-283.
- Fruchter J. S., Rancitelli L. A. and Perkins R. W. (1976) Recent and
long-term mixing of the lunar regolith based on ²²Na and ²⁶Al
measurements in Apollo 15, 16 and 17 deep drill stems and drive
tubes. Proc. Lunar Sci. Conf. 7th, 27-39.
- Hawke B. R. and Ehmann W. D. (1976) Mixing model studies of the Apollo 17
regolith. Lunar Sci. VII, 351-353.
- Irving A. J. (1975) Chemical, mineralogical and textural systematics of
non-mare melt rocks: Implications for lunar impact and volcanic
processes. Proc. Lunar Sci. Conf. 6th, 363-394.
- Korotev R. L. (1976) Geochemistry of grain-size fractions of soils from
the Taurus-Littrow Valley floor. Proc. Lunar Sci. Conf. 7th,
695-726.

- Longhi J., Walker D., Grove T. L., Stolper E. M. and Hays J. F. (1974)
The petrology of the Apollo 17 mare basalts. Proc. Lunar
Sci. Conf. 5th, 447-469.
- LSPET (1973) Apollo 17 preliminary science report. JSC SP-330, 7-25
to 7-37.
- McCallum I. S., Mathez E. A., Okamura F. P. and Ghose S. (1974) Petro-
logy and crystal chemistry of poikilitic anorthositic gabbro
77017. Proc. Lunar Sci. Conf. 5th, 287-302.
- Papike J. J., Bence A. E., Cameron K. L., and Delano J. (1973) Petrology
of the 2-4 mm soil fragments from Apollo 17. EOS, 54, 601-603.
- Papike J. J., Bence A. E., and Lindsley D. H. (1974) Mare basalts from
the Taurus-Littrow region of the moon. Proc. Lunar Sci. Conf.
5th, 471-504.
- Papike J. J., Hodges F. N., Bence A. E., Cameron M. and Rhodes J. M. (1976)
Mare basalts: Crystal chemistry, mineralogy and petrology.
Rev. Geophysics and Space Physics 4, 475-540.
- Papike J. J., Lellis S. F., Becker R. and Vaniman D. T. (1977) The Apollo 17
drill core: Modal data (sections 70007, 70008, 70009). Lunar
Sci. VIII, 753-755.
- Pratt D. D., Moore C. B., and Parsons M. L. (1977) Pattern recognition
techniques applied to chemical classifications of Apollo 17
mare basalts. Lunar Sci. VIII, 790-792.
- Rhodes J. M., Rodgers K. V., Shih C., Bansal B. M., Nyquist L. E.,
Wiesmann H. and Hubbard N. J. (1974) The relationship between
geology and soil chemistry at the Apollo 17 landing site.
Proc. Lunar Sci. Conf. 5th, 1097-1117.

- Rhodes J. M., Hubbard N. J., Wiesmann H., Rodgers K. V., Brannon J. C. and Bansal B. M. (1976) Chemistry, classification and petrogenesis of Apollo 17 mare basalts. Proc. Lunar Sci. Conf. 7th, 1467-1489.
- Ridley J. and Adams M. (1976) Petrologic studies of poikiloblastic textured rocks. Lunar Sci. VII, 739-740.
- Schaeffer O. A., Husain L. and Schaeffer G. A. (1976) The duration of volcanism in Mare Serenitatis. Earth Planet Sci. Letters, 31, 358-368.
- Schonfeld E. (1975) A model for the lunar anorthositic gabbro. Proc. Lunar Sci. Conf. 6th, 1375-1384.
- Shih C., Haskin L. A., Wiesmann H., Bansal B. M. and Brannon J. C. (1975) On the origin of high-Ti mare basalts. Proc. Lunar Sci. Conf. 6th, 1255-1285.
- Simonds C. H. (1973) Sintering and hot pressing of Fra Mauro composition glass and the lithification of lunar breccias. Amer. Jour. Sci. 273, 428-439.
- Simonds C. H., Warner J. L. and Phinney W. C. (1976) Thermal regimes in cratered terrain with emphasis on the role of impact melt. Amer. Mineralogist, 61, 569-577.
- Taylor G. J., Keil K. and Warner R. D. (1977) Very low-Ti mare basalts. Geophys. Res. Letters,

- Usselman T. M. and Lofgren G. E. (1976) The phase relations, textures, and mineral chemistries of high-titanium mare basalts as a function of oxygen fugacity and cooling rate. Proc. Lunar Sci. Conf. 7th, 1345-1363.
- Vaniman D. T. and Papike J. J. (1977a) The Apollo 17 drill core: Chemistry and stratigraphy of monomineralic fragments and the discovery of a new very low Ti (VLT) mare basalt. Lunar Sci. VIII, 952-954.
- Vaniman D. T. and Papike J. J. (1977b) Very low Ti (VLT) basalts: A new mare rock type from the Apollo 17 drill core. Proc. Lunar Sci. Conf. 8th.
- Vaniman D. T. and Papike J. J. (1977c) The Apollo 17 drill core: Modal petrology and glass chemistry (sections 70007, 70008, 70009). Proc. Lunar Sci. Conf. VIII.
- Walker D. , Longhi J., Grove T. L., Stolper E. and Hays J. F. (1973) Experimental petrology and origin of rocks from the Descartes Highlands. Proc. Lunar Sci. Conf. 4th, 1013-1032.
- Warner J. L., Simonds C. H. and Phinney W. C. (1973) Apollo 16 rocks: Classification and petrogenetic model. Proc. Lunar Sci. Conf. 4th, 481-504.
- Warner J. L., Simonds C. H., Phinney W. C., Geeslin J. H., and Bickel C. E. (1977) Petrology and crystallization history of Apollo 14 impactites. Lunar Sci. VIII, 982-984.

Warner R. D., Keil K., Prinz M., Laul J. C., Murali A. V. and Schmitt
R. A. (1975) Mineralogy, petrology and chemistry of mare
basalts from Apollo 17 rake samples. Proc. Lunar Sci. Conf.
6th, 193-220.

Wolfe E. W., Luchitta B. K., Reed V. S., Ulrich G. E. and Sanchez A. G.
(1975) Geology of the Taurus-Littrow Valley floor. Proc. Lunar
Sci. Conf. 6th, 2463-2482.

